Semiconductor Ring Laser dynamics

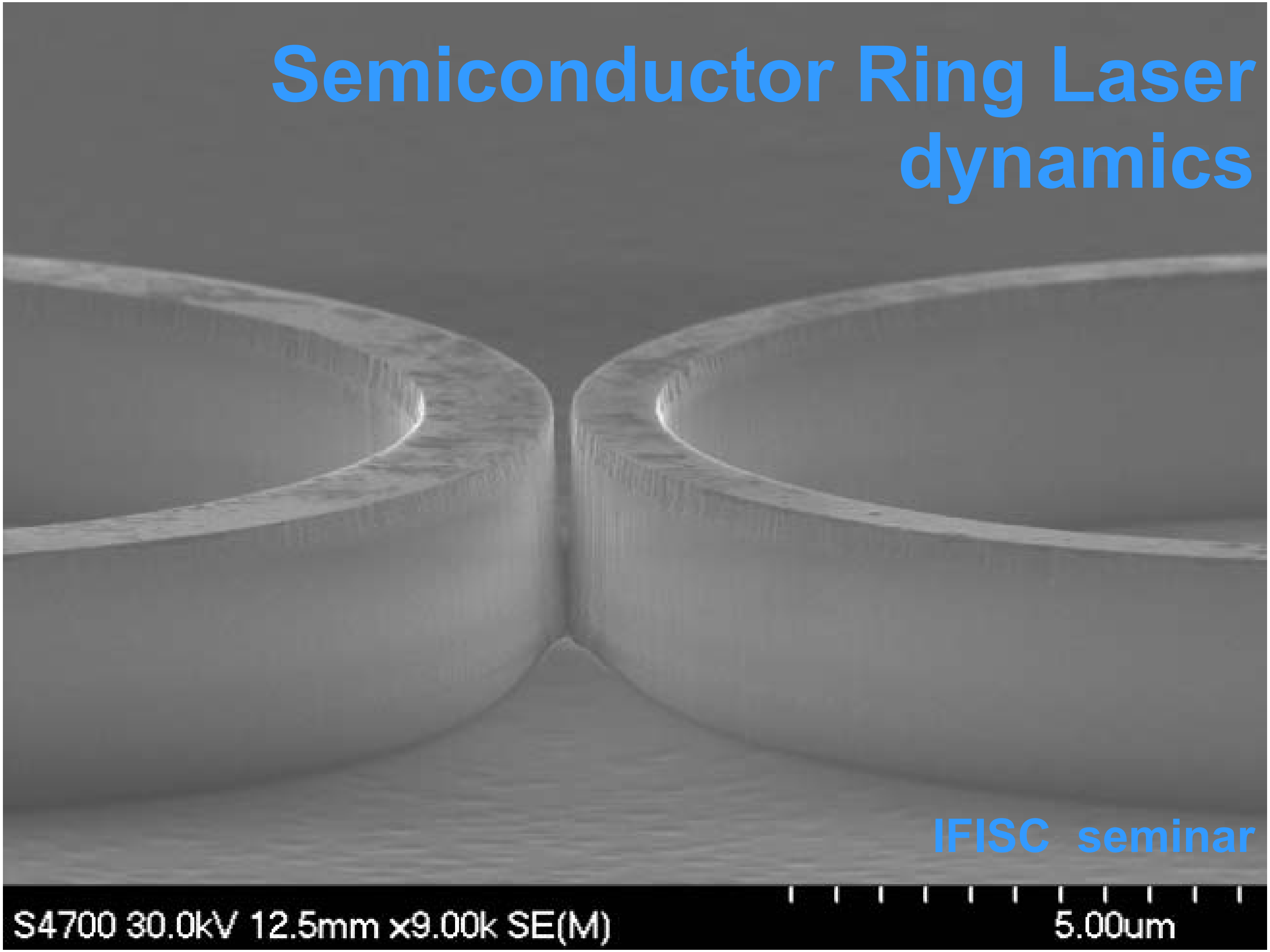

IFISC seminar

- Introduction
- Basic properties (directional bistability)
- Modal Properties
- TW-modelling
- Directional switching
- Noise properties
    - *Langevin formulation, noise spectra*
    - *Mode hopping*
- Applications
    - *Inertial rotation sensing*
    - *Hardware Random Number Generation*
- New structures
    - *Snail laser*
    - *Active Photonic Molecules*
- Conclusions

Sources of light

- **Natural**
- **Direct chemical**
- **Combustion-based**
- **Electric powered**
- **Incandescent lamps**
- **Electroluminescent lamps**
- **Gas discharge lamps**
- **High-intensity discharge lamps**
- **LASER**

- *Gas lasers*
- *Chemical lasers*
- *Dye lasers*
- *Metal-vapor lasers*
- *Solid-state lasers*
- ***Semiconductor lasers***
- *X-rays*

- ***Edge-emitter***
- ***Vertical Cavity***
- ***Ring***

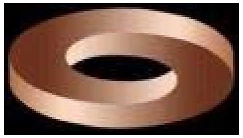

Semiconductor Laser. Working principle

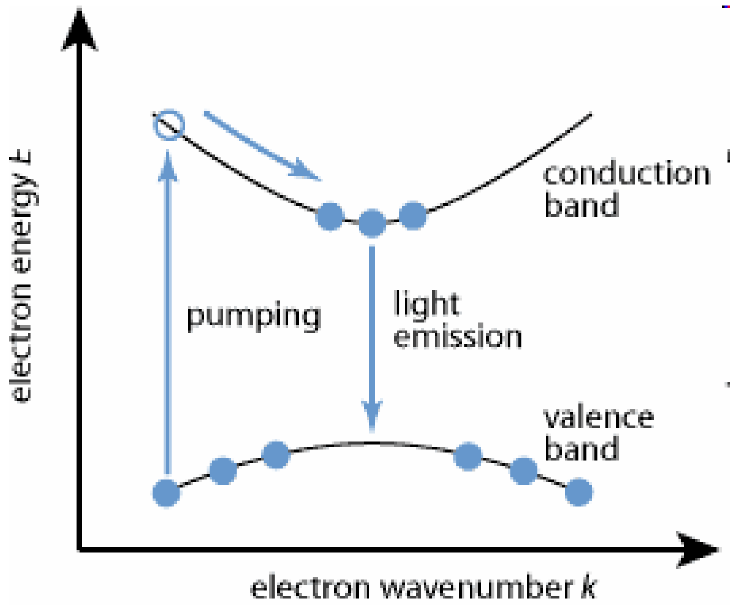

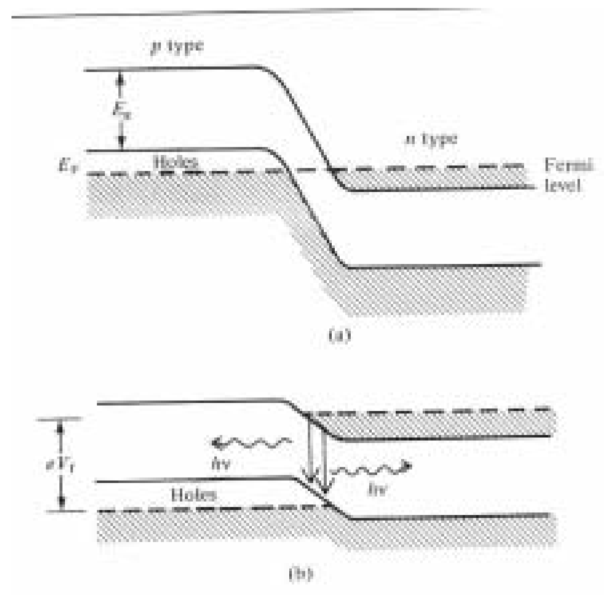

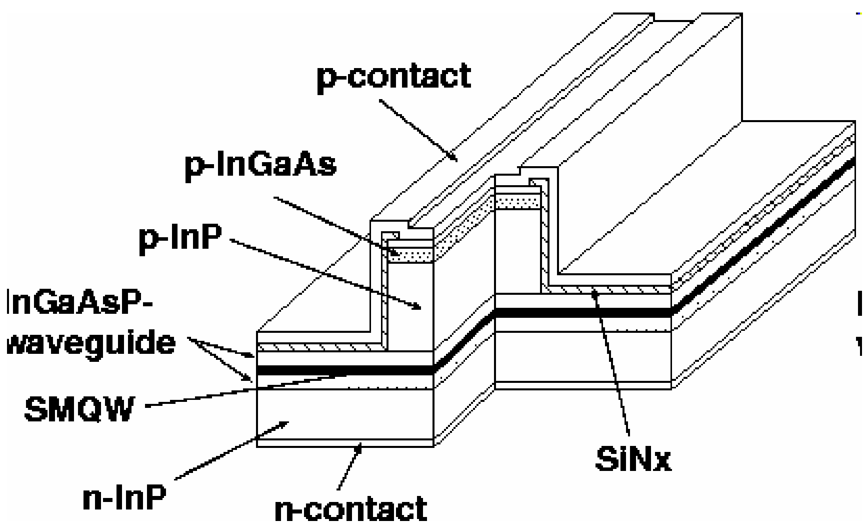

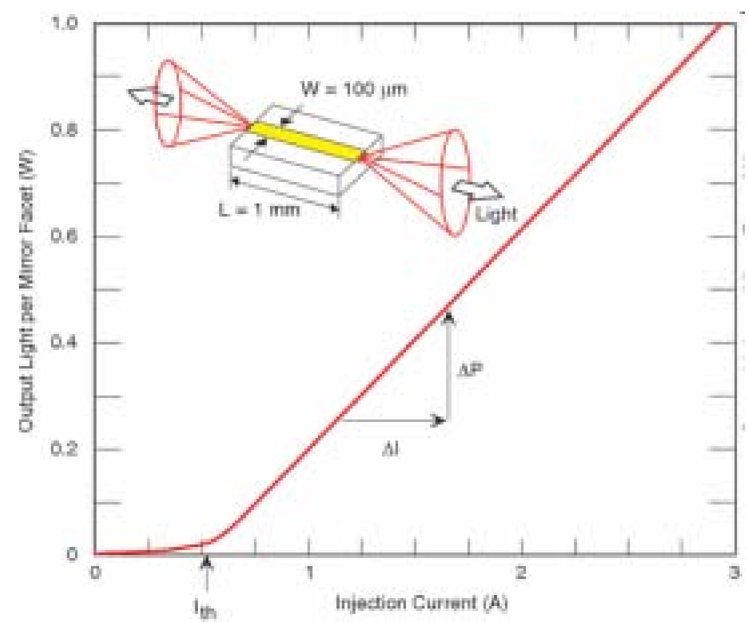

- Research
  - Multimode properties
  - Non-linear dynamics
  - ….

- Applications
  - Telecom
  - Data storage/reading
  - Measuring instruments
  - Laser absorption spectrometry
  - ….

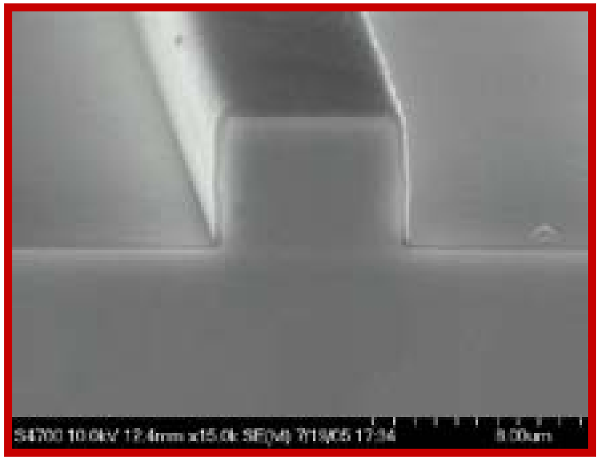

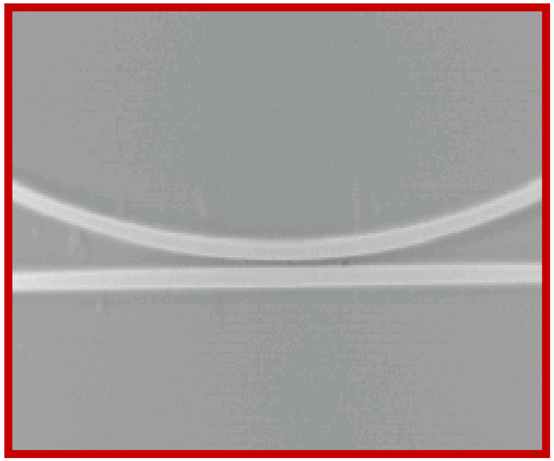

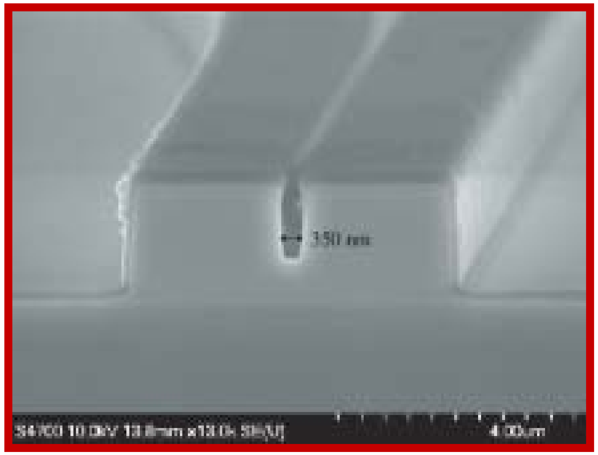

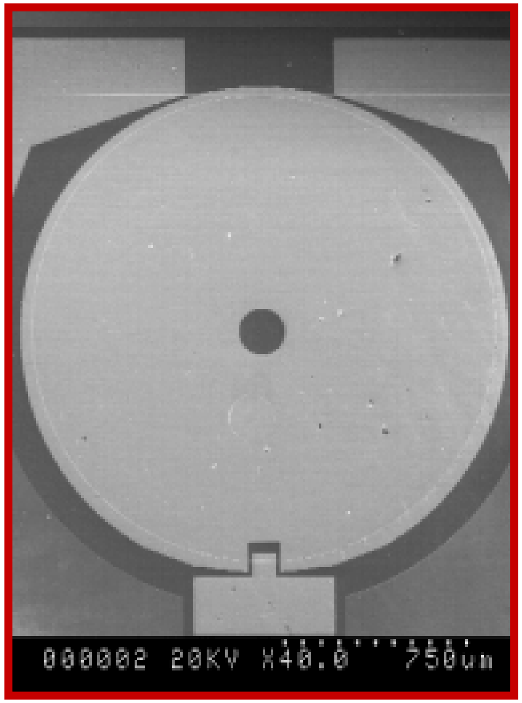
000002 20KV X40.0 750um

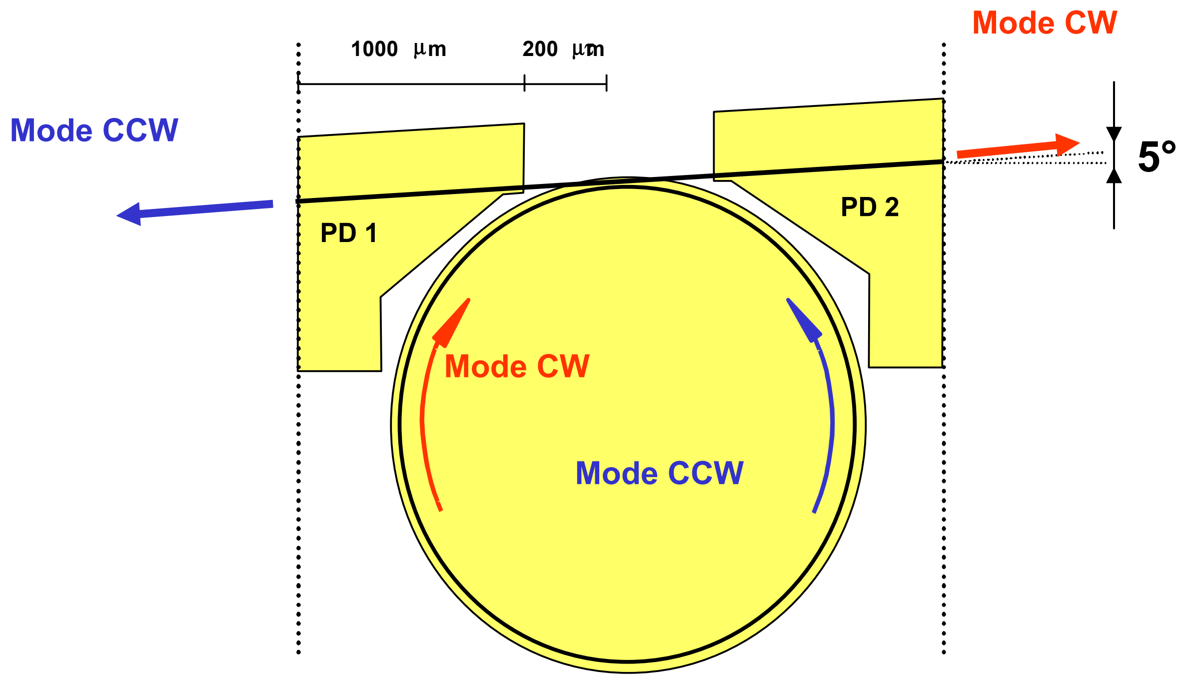
1000 µm
200 µm
Mode CW
Mode CCW
5°
PD 1
PD 2
Mode CW
Mode CCW

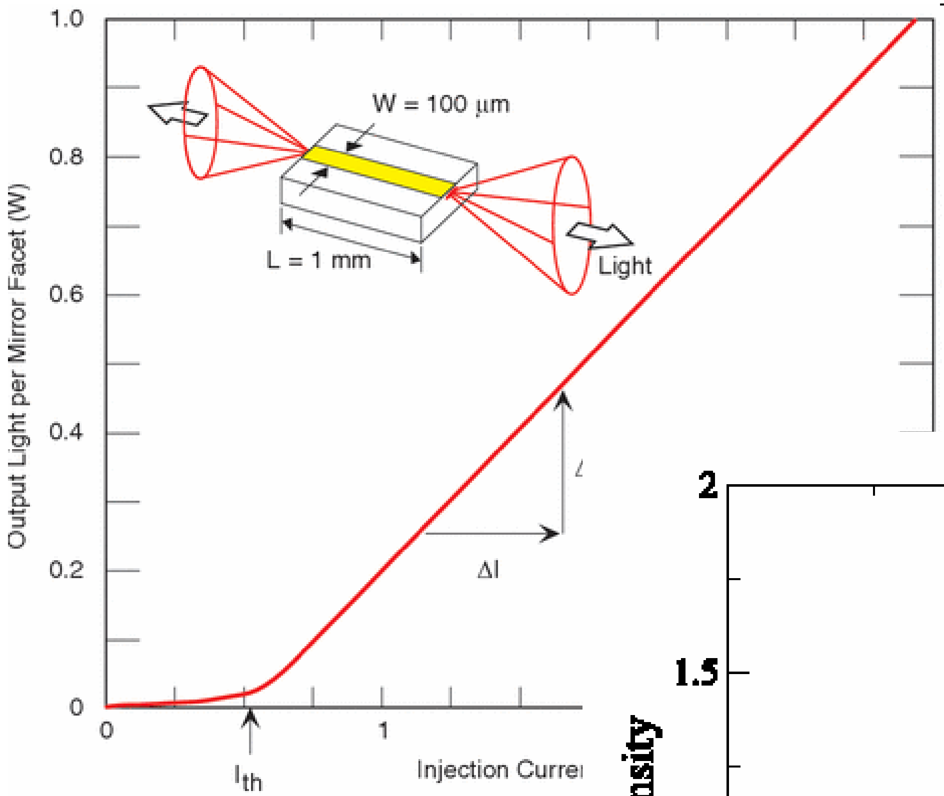
Output Light per Mirror Facet (W)
1.0
0.8
0.6
0.4
0.2
0
0
1
I_th
Injection Curre
W = 100 µm
L = 1 mm
Light
ΔI

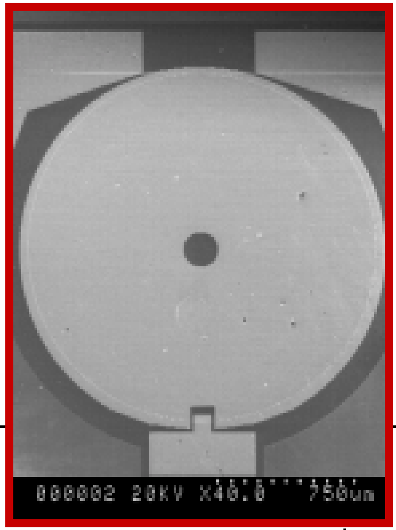
000002 20KV X40.0 750um

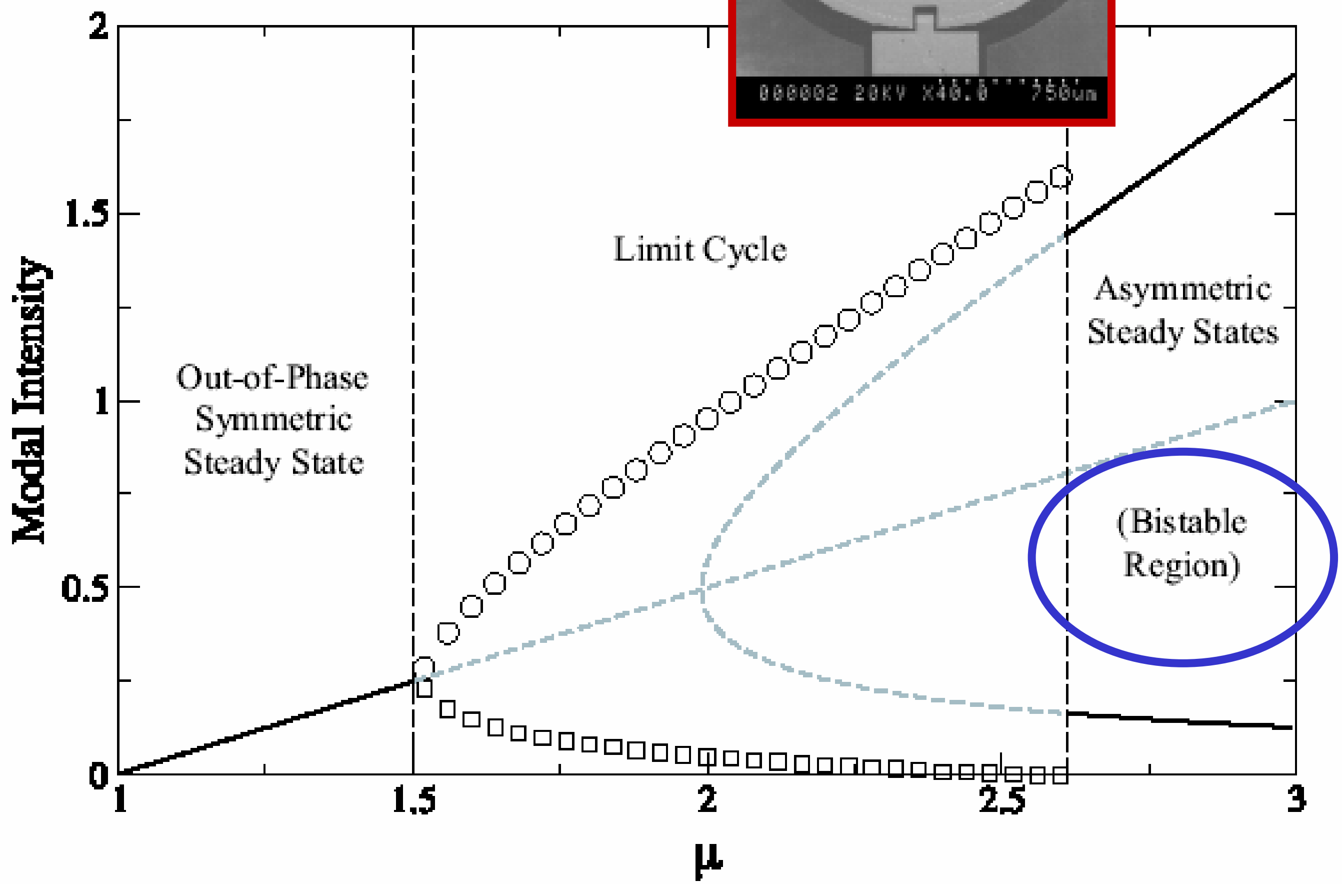
Modal Intensity
μ
0
0.5
1
1.5
2
1
1.5
2
2.5
3
Out-of-Phase
Symmetric
Steady State
Limit Cycle
Asymmetric
Steady States
(Bistable
Region)

SIXTH FRAMEWORK PROGRAMME

FP6-2005-IST-5

PRIORITY 2 - INFORMATION SOCIETY TECHNOLOGIES

Contract for:

SPECIFIC TARGETED RESEARCH PROJECT

Annex I - "Description of Work"

Project acronym: IOLOS

Project full title: Integrated Optical Logic and Memory using Ultra-fast Micro-ring Bistable Semiconductor Lasers

Proposal/Contract no.: 34743

- *"Development of Theoretical Model and Simulation Tools for SRL bistable device: develop theoretical framework and numerically implement mathematical models to provide understanding and guidance for the design and optimisation of the bistability and switching speed of micro-SRLs."*

Partic. Role*	Partic. no.	Participant name	Participant short name	Country
CO	1	University of Bristol	UNIVBRIS	UK
CR	2	University of Glasgow	GU	UK
CR	3	Università degli Studi di Pavia	UNIPV	Italy
CR	4	Universitat de les Illes des Balears	UIB	Spain
CR	5	Vrije Universiteit Brussel	VUB	Belgium
CR	6	Intense Ltd	Intense	UK
CR	7	Siemens SA	Siemens	Portugal

University of BRISTOL

VRIJE UNIVERSITEIT BRUSSEL • SCIENTIA VINCERE TENEBRAS •

UNIVERSITY of GLASGOW

PUBLICATIONS

MODAL STRUCTURE, DIRECTIONAL AND WAVELENGTH JUMPS OF INTEGRATED SEMICONDUCTOR RING LASERS: EXPERIMENT AND THEORY

Fürst, Sandor; Pérez-Serrano, Antonio; Scirè, Alessandro; Sorel, Marc; Balle, Salvador
Applied Physics Letters 93, 251109 , (2008)

■ Modes in a Ring Cavity

Electric field:

$$E(z,\omega) = A_F(\omega)e^{iq(\omega)z} + A_B(\omega)e^{-iq(\omega)z}$$

Boundary conditions:

$$\begin{cases} A_F = RA_B + TA_F e^{iq(\omega)L} \\ A_B e^{-iq(\omega)L} = RA_F e^{iq(\omega)L} + TA_B \end{cases}$$

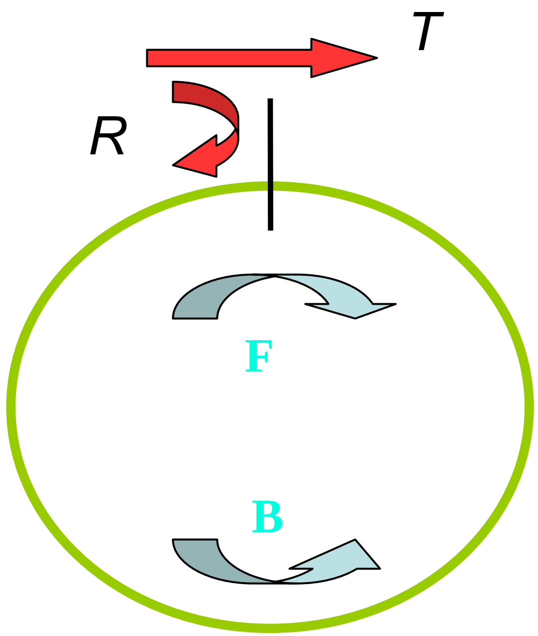

Ideal ring ($R = 0$, $T = 1$) :

$$q = \frac{2\pi m}{L} \qquad m = 0, \pm 1, \pm 2, \ldots$$

General case ($R \neq 0$, $T \neq 0$) :

$$q_\pm = \frac{2\pi m}{L} + \frac{i}{L}\ln(T \pm R) \qquad m = 0, \pm 1, \pm 2, \ldots$$

Two branches of solutions

■ Theoretical Analysis

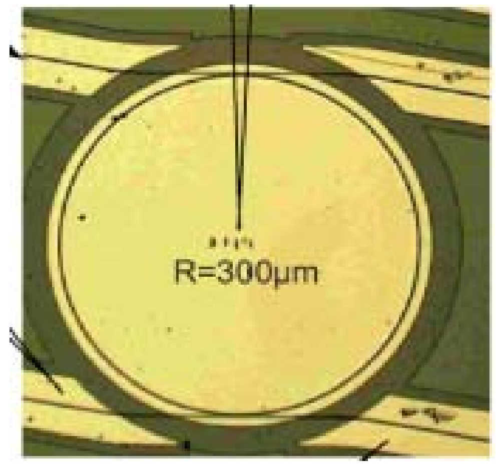

Round Trip Condition: $$e^{2iqL} - ae^{iqL} + b = 0$$

$$b = (r_u r'_u - t_u t'_u)^{-1}(r_d r'_d - t_d t'_d)^{-1} \qquad a = (r_u r_d + r'_u r'_d + t'_u t_d + t_u t'_d)\, b$$

Modes: $$q_m^{\pm} L = 2\pi m - i \ln Q_{\pm} \qquad Q_{\pm} = a/2 \pm [(a/2)^2 - b]^{1/2}$$

Splitting: $$\Delta = \frac{1}{2\pi}\left\{ \mathrm{Im}\left[\ln\left(\frac{Q_-}{Q_+}\right)\right] - \alpha\, \mathrm{Re}\left[\ln\left(\frac{Q_-}{Q_+}\right)\right]\right\}$$

■ Experimental Setup

- Wafer: Multiple QW AlGaInAs/InP structure grown by MOCVD.

- Waveguides defined by electron beam lithography and transferred to a PECVD SiO_2 layer, using CHF_3 RIE.

- Shallow etched ridge-waveguide defined by RIE, using CH_4 / H_2 / O_2 process.

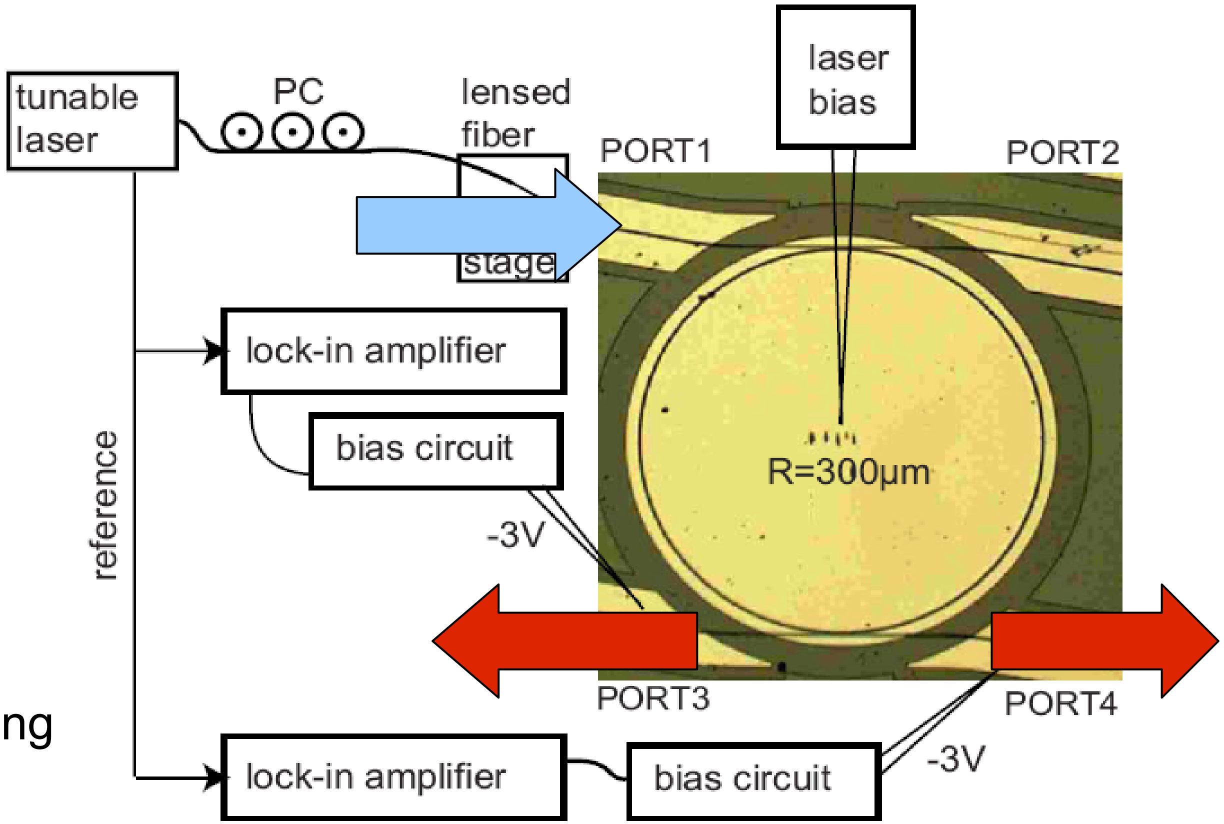

- Deposition of SiO_2 layer and contact window definition

- Metal contacts deposited on epitaxial and substrate sides of the wafer section.

Experimental

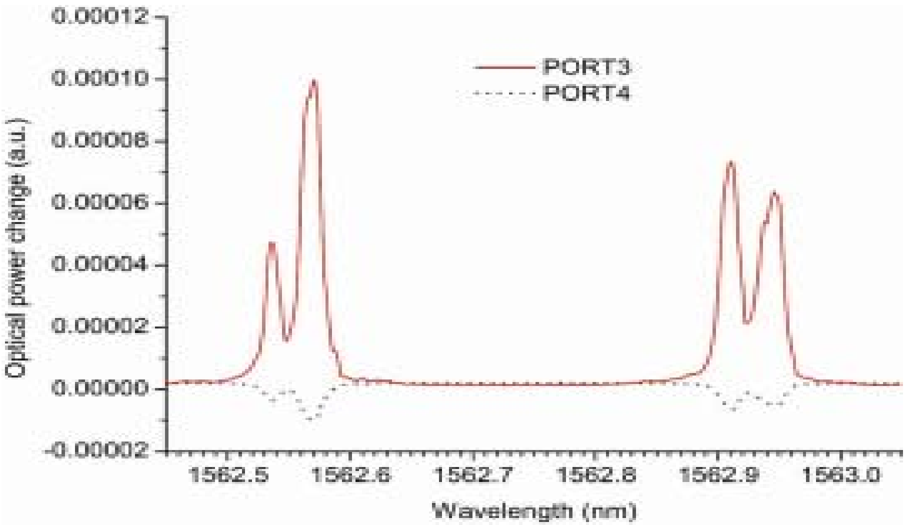

Theoretical

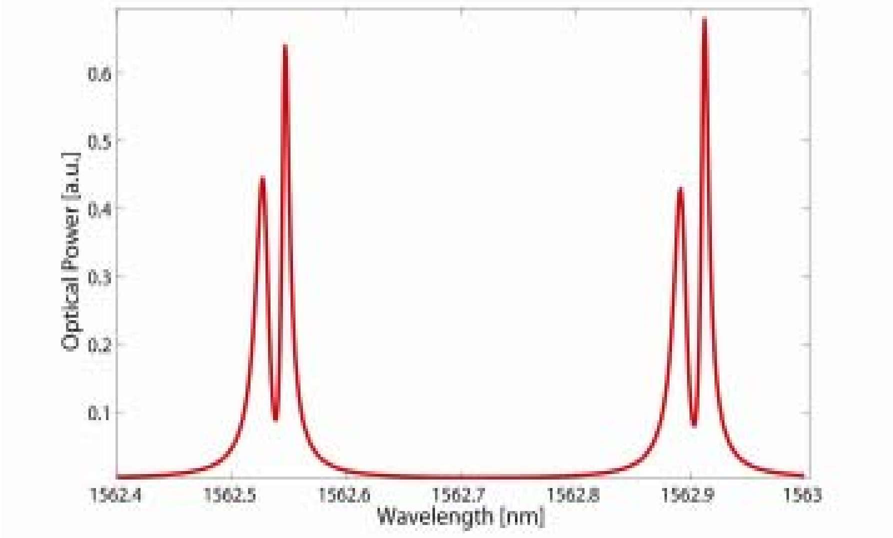

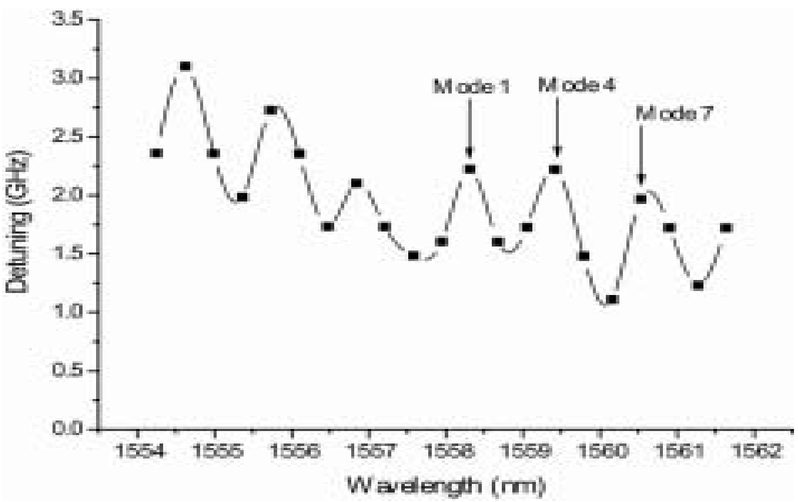

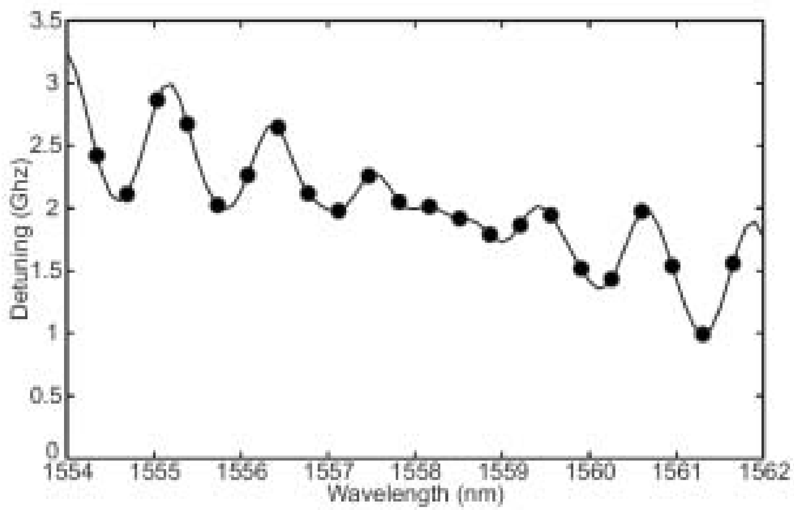

Ultrafast All-Optical Switching of Bistable Semiconductor Ring Lasers

***J. Javaloyes*[1], *A. Trita*[2], *G. Mezosi*[1], *F. Bragheri*[2], *I. Cristiani*[2], *G. Giuliani*[2], *M. Sorel*[1], *A.Scirè*[3] *and S. Balle*[4]**

1. *Dept. of Electronics and Electrical Engineering, U. of Glasgow, Rankine Building, Oakfield Avenue, Glasgow G12 8LT, UK*
2. *Dip. di Elettronica, Università di Pavia, I-27100 Pavia, Italy*
3. *Instituto de Física Interdisciplinar y Sistemas Complejos (CSIC-UIB), Ctra. Valldemossa km. 7'5, E-07122 Palma de Mallorca, Spain*
4. *Institut Mediterrani d'Estudis Avançats (CSIC-UIB), C/. Miquel Marqués 21, E-07190 Esporles, Spain*

Laser description. Active medium.

Medium Polarization:

$$\mathcal{P} = \varepsilon_0 \Gamma_x \chi(\omega, N) E(z, \omega)$$

Lorentzian Susceptibility:

$$\chi(\omega, N) = \frac{\chi_0 N}{\omega - \omega_0 + i\gamma}$$

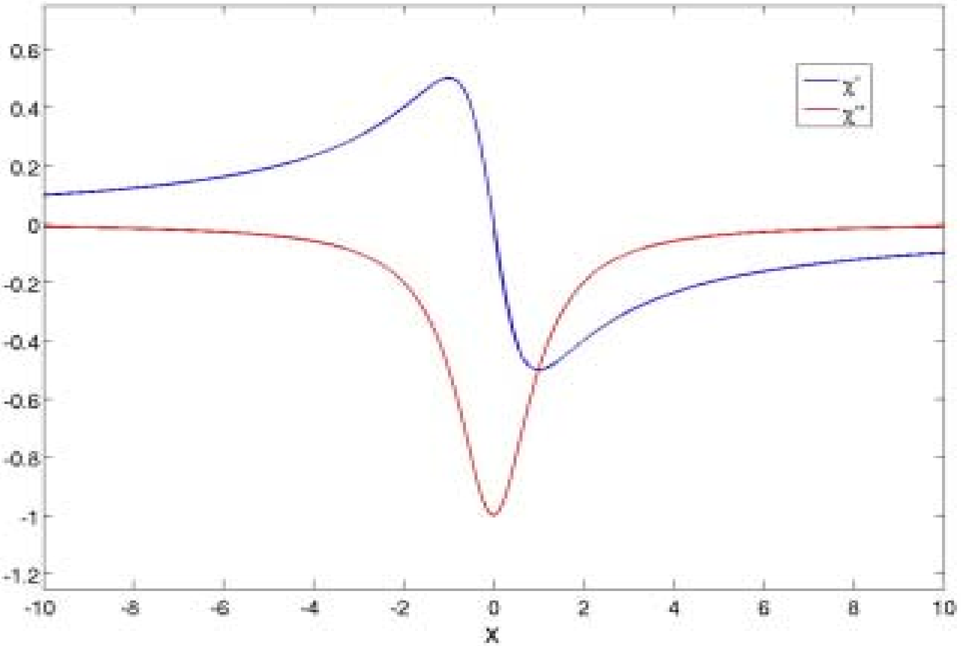

x

- Quasimonochromatic approximation

$$A(z, \omega) \sim \delta(\omega - \Omega)$$

- Slowly varying amplitude approximation

$$\lambda^2 \frac{\partial^2 A_{B,F}}{\partial z^2} \ll \lambda \frac{\partial A_{B,F}}{\partial z} \ll A_{B,F}$$

$$\lambda \frac{\partial A_{B,F}}{\partial z} \sim 0$$

- Analytic optical susceptibility from equilibrium many-body theory for Quantum-Well semiconductor lasers
- Nonlinear dependence on the carrier density, providing both a broad gain spectrum and a dispersion curve, "*so it can be used to analyze the dynamics of multimode devices or devices with large carrier density variations*".
- *[S.Balle – Phys. Rev. A **37** 1304 (1999)]*

$$\chi_E(\omega) = -\frac{i}{\varepsilon_0}\frac{2}{V}\sum_{l,m}\sum_{k}|M_{lm}(k)|^2 \times \frac{f_l(k) - f_m(k)}{i[E_{lm}(k) - \hbar\omega] + \hbar\gamma(k)},$$

$$\chi(\omega, N) = -\chi_0\left[2\ln\left(1 - \frac{D}{u+i}\right) - \ln\left(1 - \frac{b}{u+i}\right)\right], \qquad (6)$$

$$\chi_0 = \frac{m|M|^2}{W\pi\varepsilon_0\hbar^2}, \quad D = \frac{\pi W\hbar}{m\gamma}N \equiv \frac{N}{N_t},$$

$$u = \frac{Re(z)}{\gamma} = \frac{(\omega - E_t/\hbar)}{\gamma}, \quad b = \frac{\hbar k_m^2}{2m\gamma}.$$

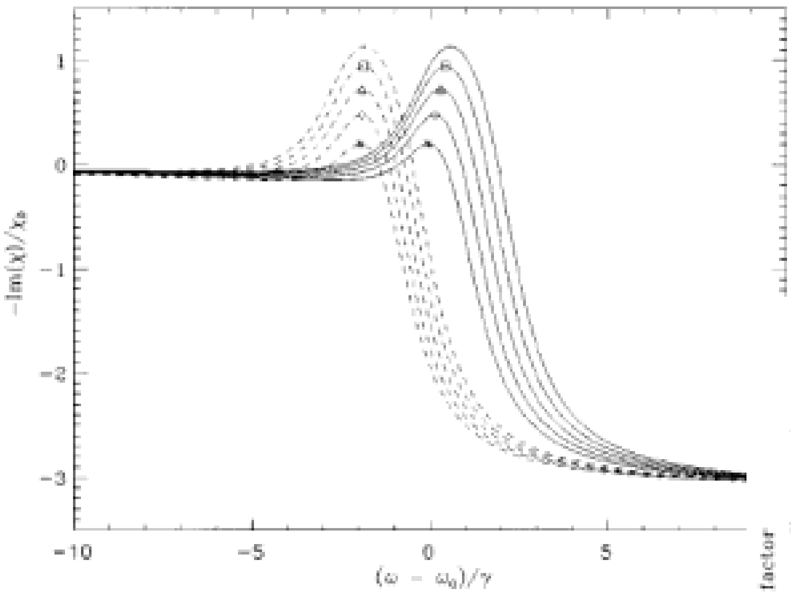

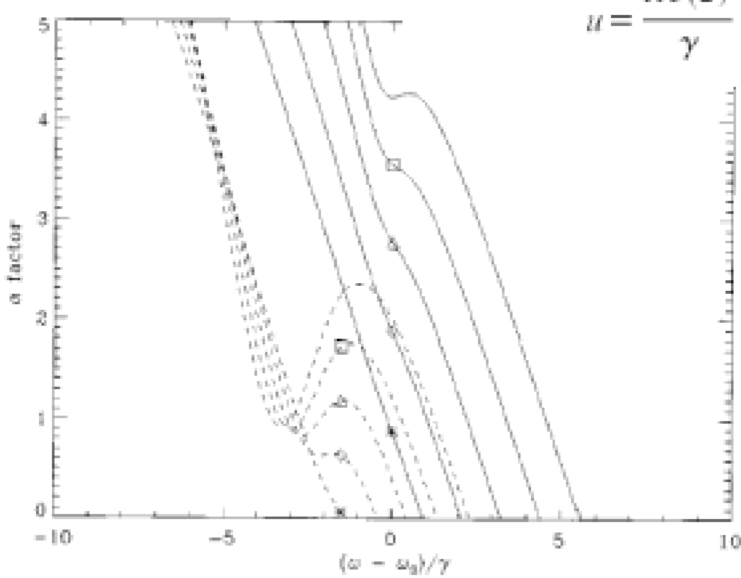

Directional switching in Semiconductor Ring Laser induced by pulse injection

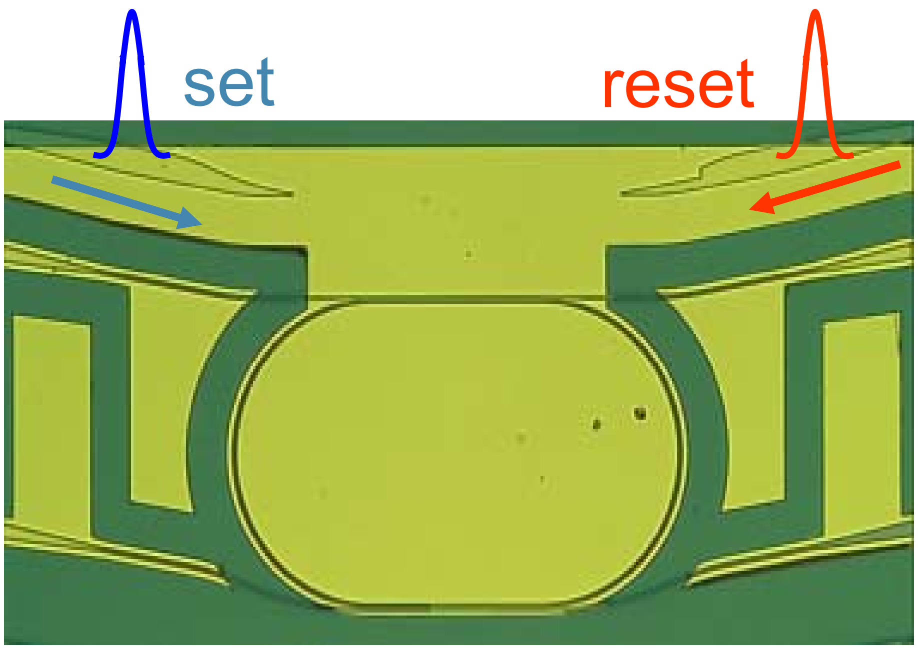

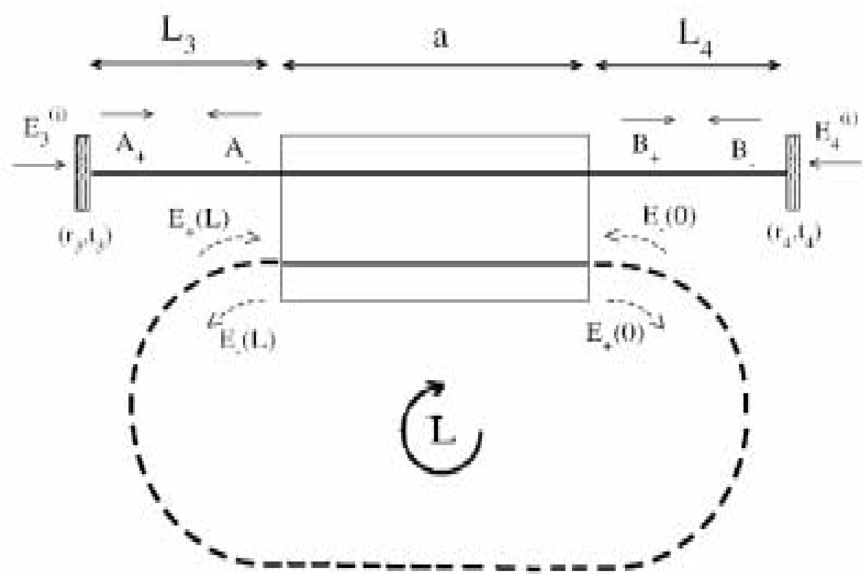

18 ps round trip

$$\mathcal{E}(x,y,z,t)=\left[A_+(z,t)e^{iq_0z}+A_-(z,t)e^{-iq_0z}\right]\times\Phi(x,y,\omega_0)e^{-i\omega_0t}+\text{c. c.}$$

$$N(z,t)=N_0(z,t)+\left[N_2(z,t)\,e^{2iq_0z}+\text{c. c.}\right]+\cdots$$

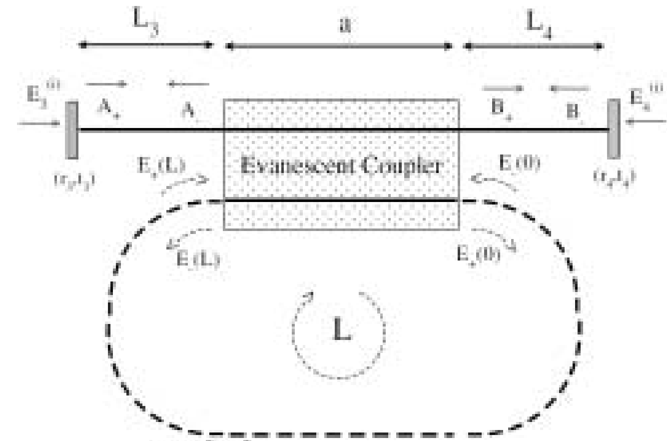

$$\left(\pm\partial_z+\frac{1}{v_g}\partial_t\right)A_\pm=i\frac{\omega_0}{2\varepsilon_0cn}B_\pm(z,t)-\frac{\alpha_i}{2}A_\pm$$

$$\partial_tN_0=\frac{I}{eV_a}-R(N_0)+\mathcal{D}\partial_z^2N_0-\frac{2i}{\hbar S_a}(A_+^*B_++A_-^*B_--\text{c. c.})$$

$$\partial_tN_2=-\left[R'(N_0)+4\mathcal{D}q_0^2\right]N_2-\frac{2i}{\hbar S_a}(A_-^*B_+-A_+B_-^*)$$

$$\begin{aligned}ib(N_0)\partial_tB_\pm=&-B_\pm+\varepsilon_0\Gamma\left[\chi(\omega_0,N_0)A_\pm+ia(N_0)\partial_tA_\pm\right.\\&-\varepsilon g_{NL}(\omega_0,N_0)(|A_\pm|^2+2|A_\mp|^2)A_\pm\\&\left.+\chi_N(\omega_0,N_0)N_{\pm2}A_\mp\right]\end{aligned}$$

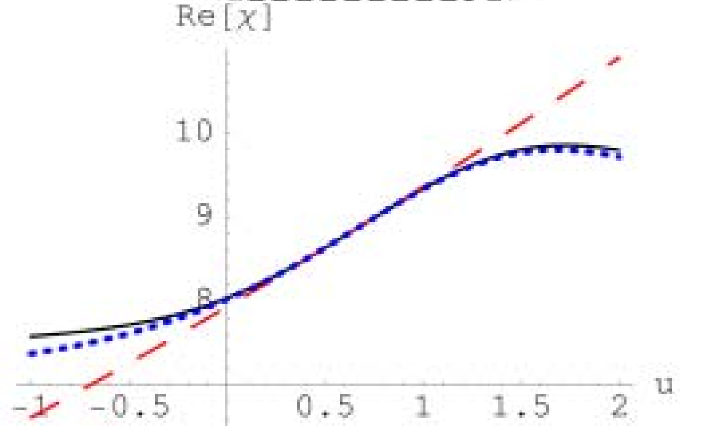

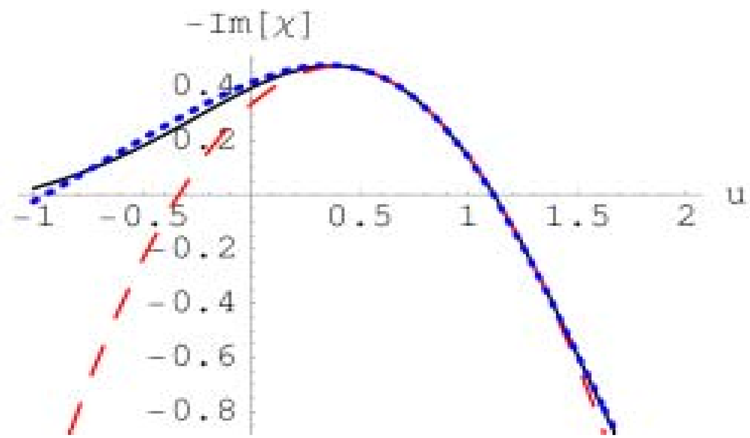

$$a(N)=\chi_\omega(\omega_0,N)+b(N)\,\chi(\omega_0,N)$$

$$b(N)=-\frac{1}{2}\frac{\chi_{\omega\omega}(\omega_0,N)}{\chi_\omega(\omega_0,N)}$$

$$g_{NL}(\omega,N)=\left[\chi(\omega,N)-c.c.\right]/4$$

Dynamics as a function of the Pulse Energy

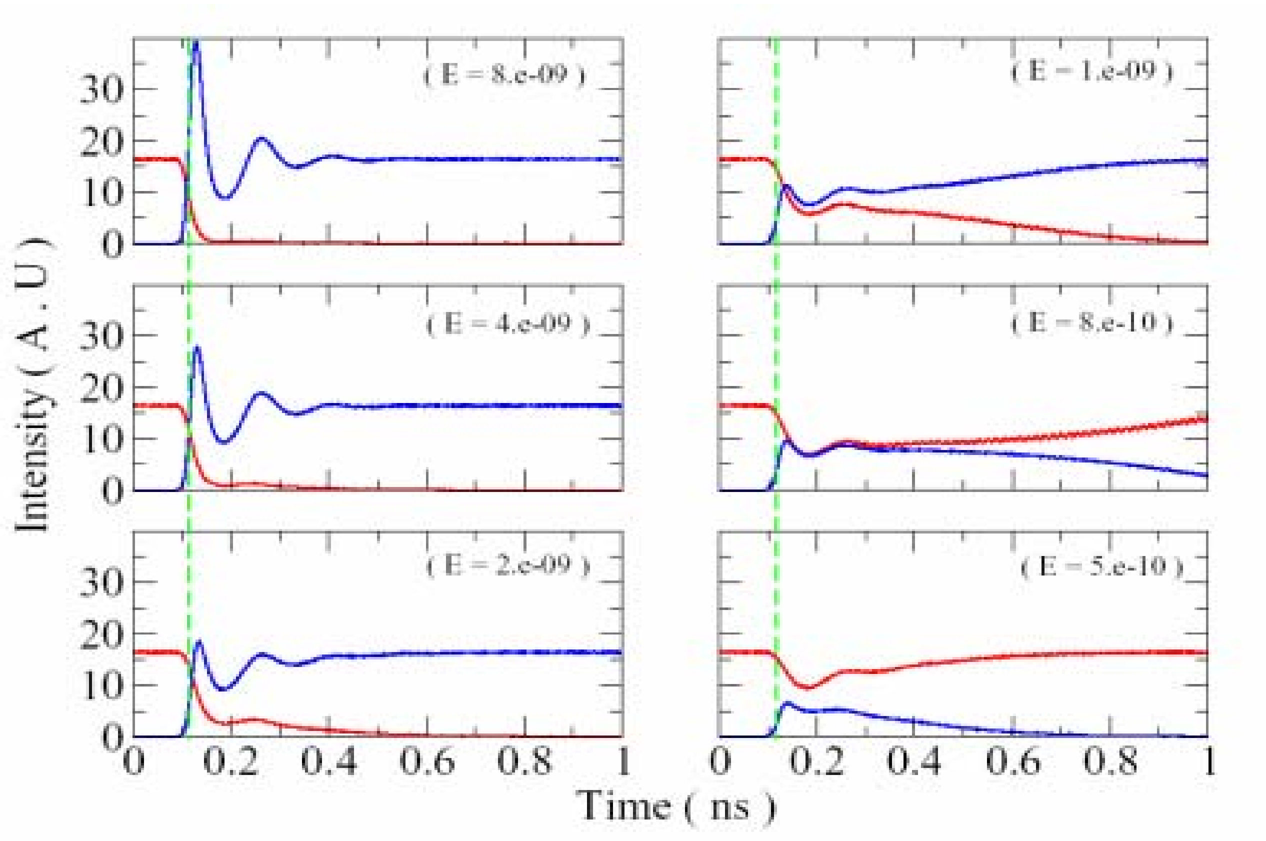

Resonant pulse , fixed FWHM (47 ps)
<u>variable Energy</u>

<u>High Pulse energy</u>

Fast switching with

relaxation oscillation

<u>Low Pulse energy</u>

No switching

Dynamics as a function of the Pulse Energy

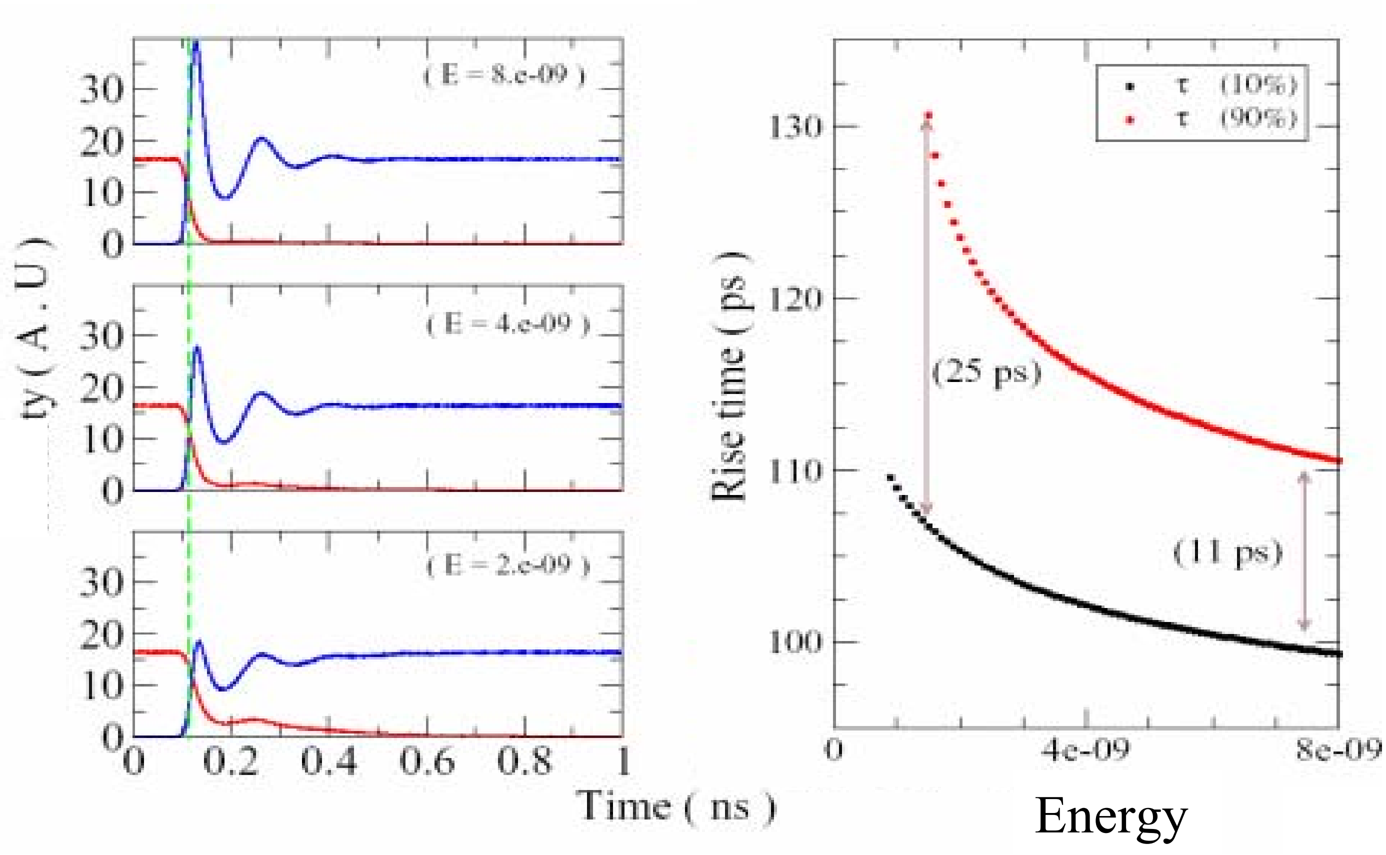

Resonant pulse , fixed FWHM (47 ps)
variable Energy

High Pulse energy

Fast switching with relaxation oscillation

Low Pulse energy

No switching

Dynamics as a function of the Pulse Energy

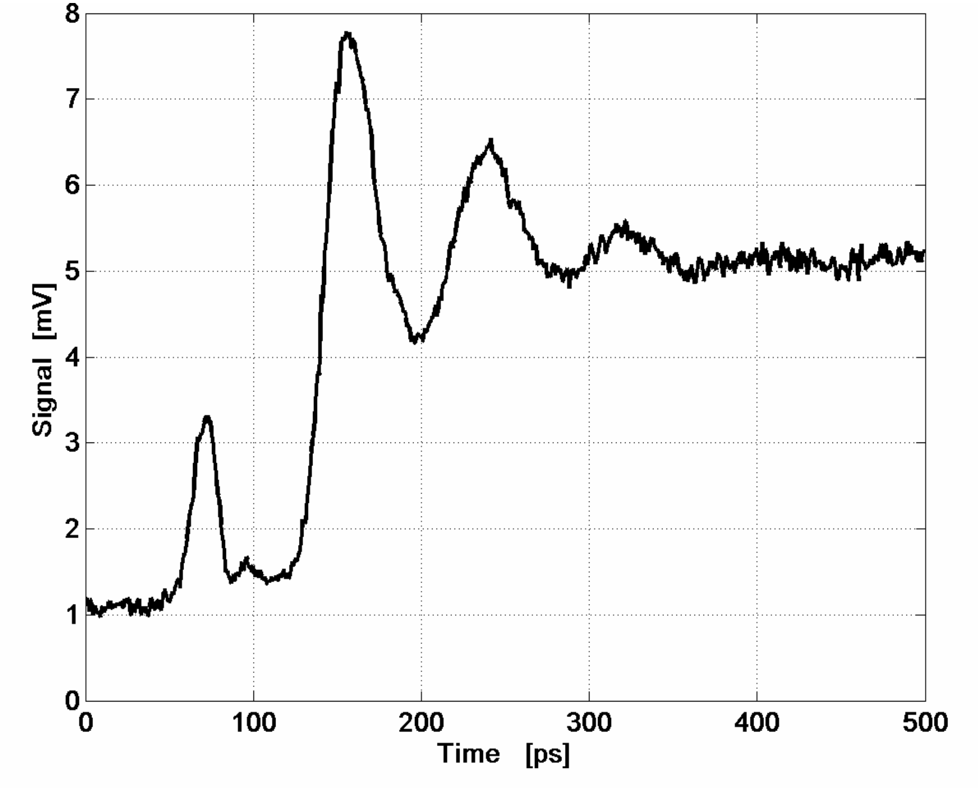

Experimental Results (5ps Pulses)

High Pulse energy

Fast switching with

relaxation oscillation

Low Pulse energy

No switching

Dynamics as a function of the Pulse width

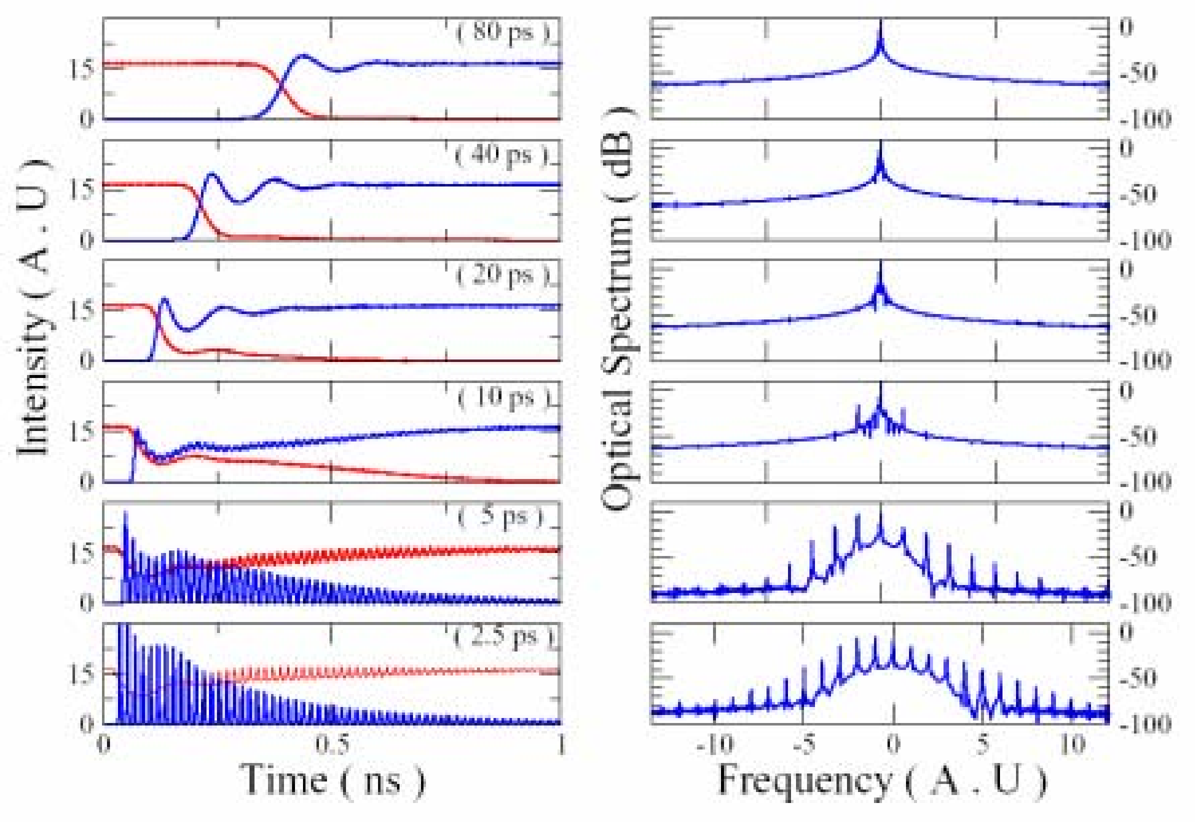

Resonant pulse , fixed Energy (2.e-09)
<u>variable FWHM</u>

<u>slow Pulse</u>

All the energy goes

into the lasing mode

<u>Fast Pulse</u>

Energy is shared

between adjacent modes

Dynamics as a function of the Pulse width

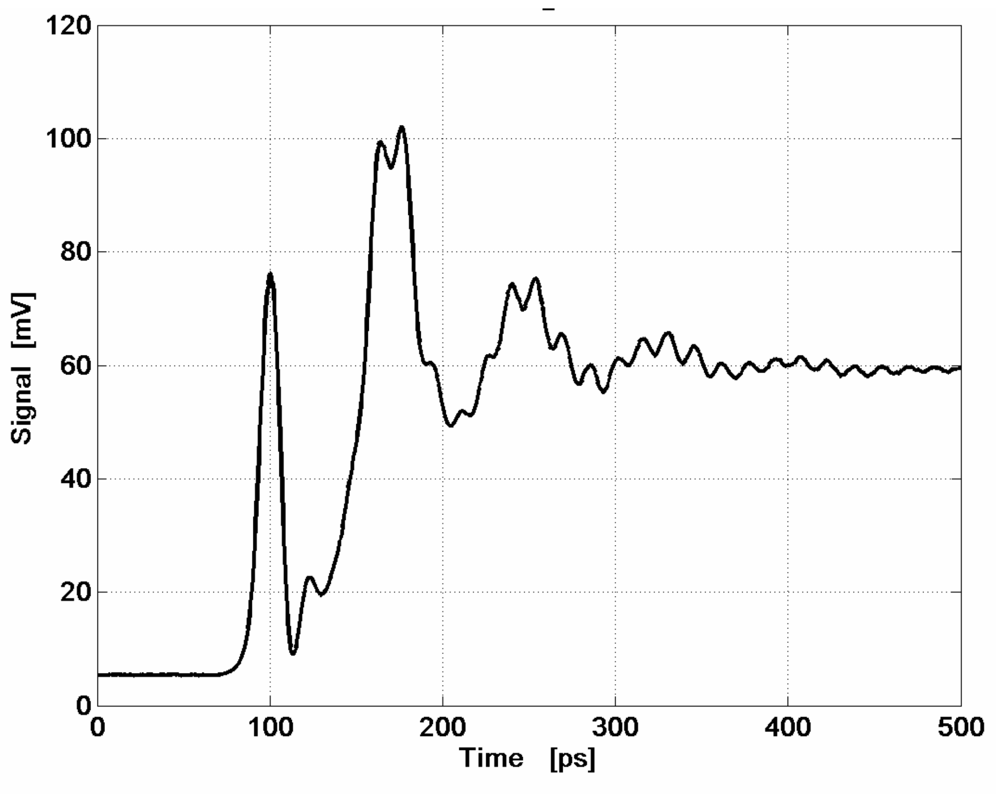

Experimental Results (5ps Pulses)

slow Pulse

All the energy goes

into the lasing mode

Fast Pulse

Energy is shared

between adjacent modes

Dynamics as a function of the pulse detuning

Fixed Energy (4.e-09)

Fixed FWHM (47 ps)

<u>Variable Detuning</u>

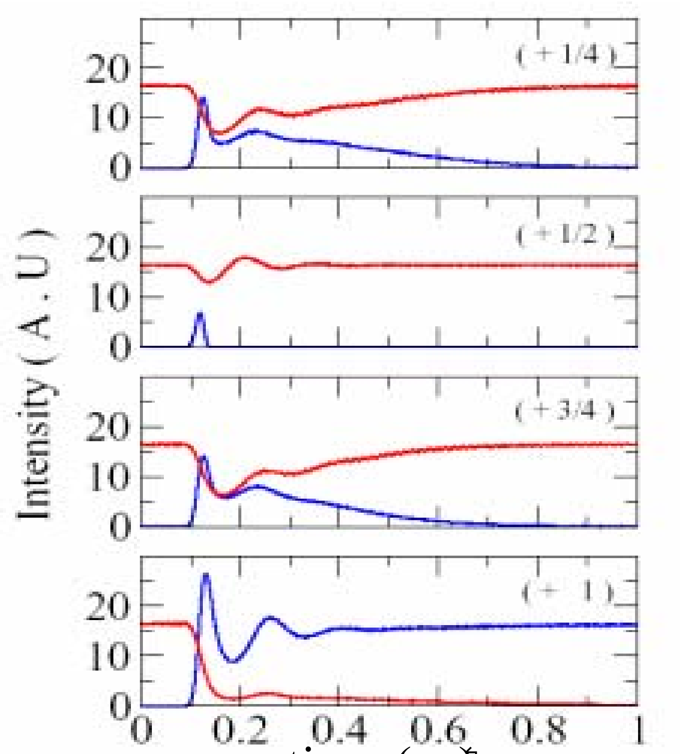

<u>Resonant Pulse</u>

All the energy goes

into the lasing mode

<u>AntiResonant Pulse</u>

Energy can not

enter the cavity

<u>To mitigate</u>

With higher energy one can switch with high detuning
With short pulses (broad spectrum), detuning is irrelevant

Dynamics of a Set-Reset operation

<u>two</u> pulses

Fixed Energy (4.e-09)

Fixed FWHM (47 ps)

<u>variable</u>
<u>set reset delay σ</u>

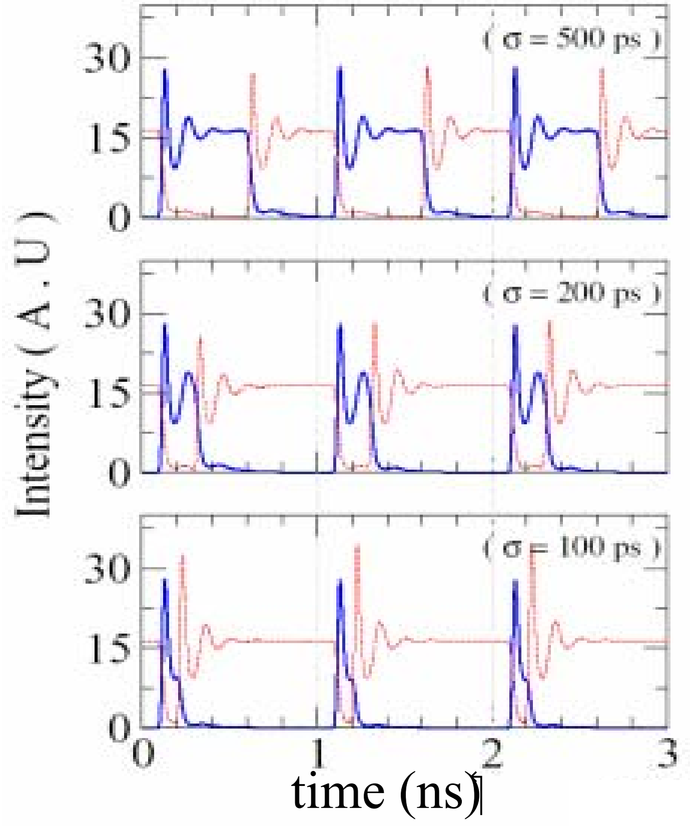

<u>Set-Reset operation</u>

is limited by the

- Rise time of the pulse
- Rise time of the laser
- High speed ⟹ Short pulse

Fast pulse response and Scaling Down Laser Size

Variable Energy

Fixed FWHM (5 ps)

Variable Laser Size
(20, 15, 10 and 5 ps)

Different conditions
but
similar ROF

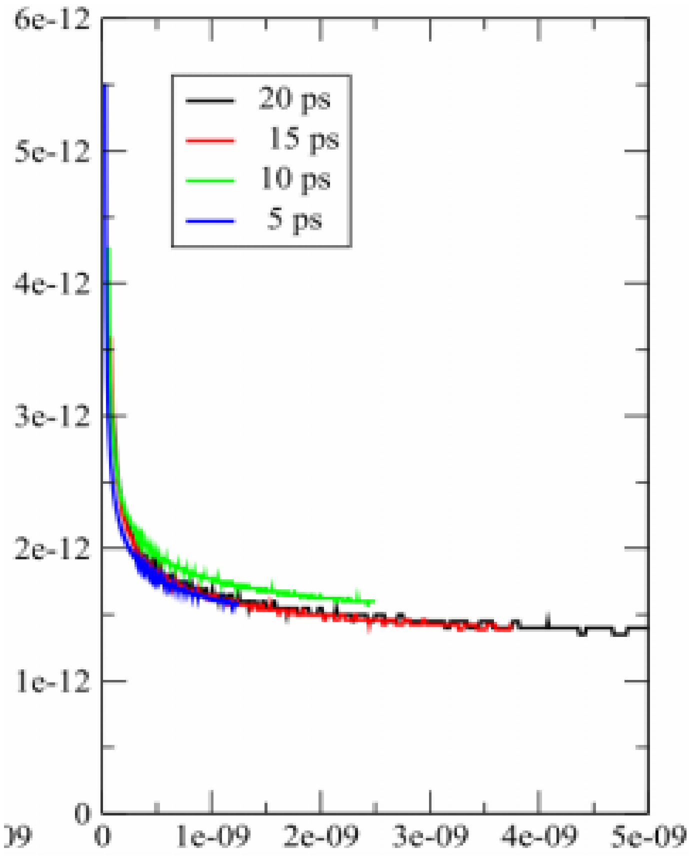

Energy

No improvment on

the rise time while

decreasing the size

Small devices are
more complicated
(thermal managment)

Fast pulse response and Scaling Down Laser Size

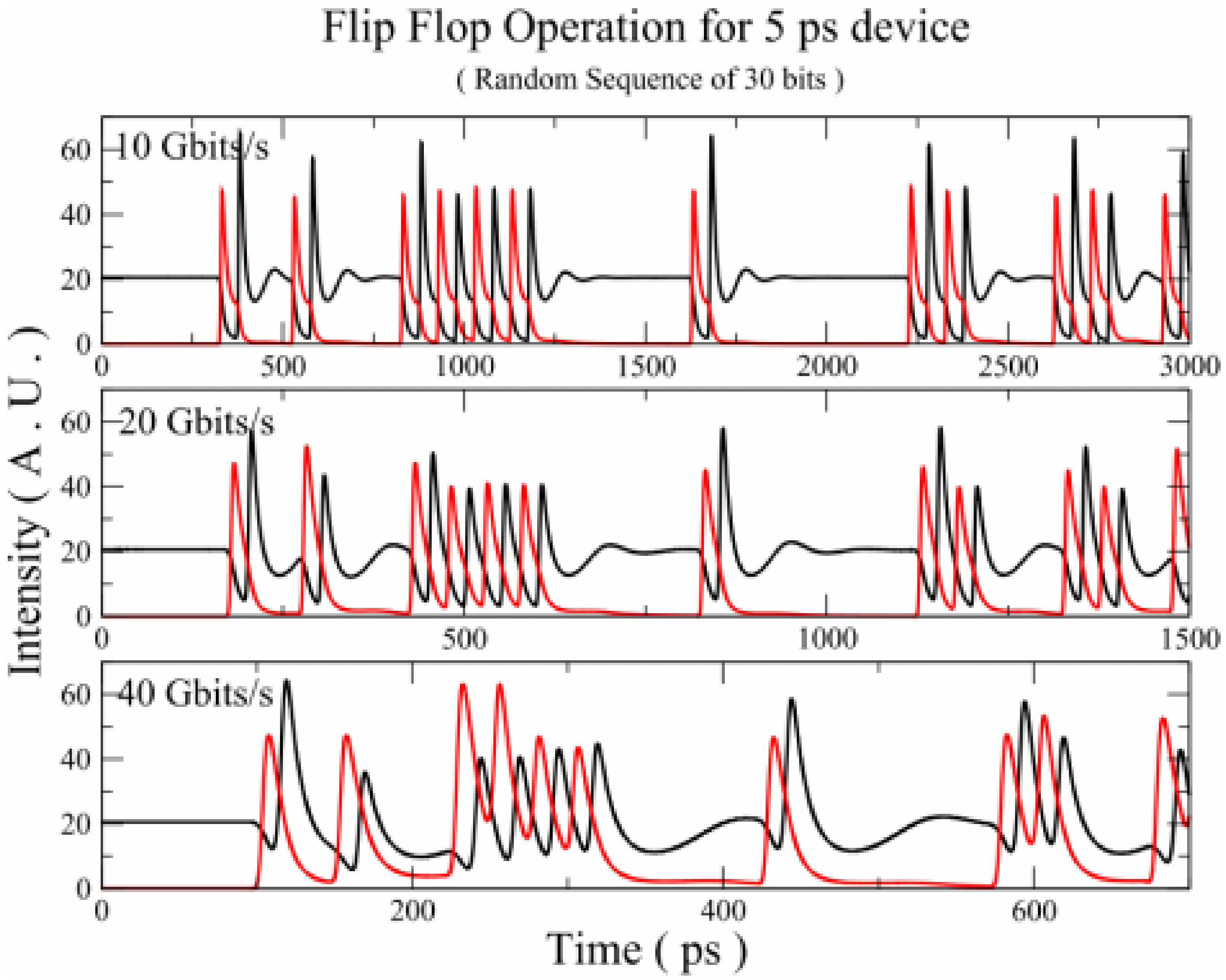

1 = Flip-Flop

0 = Nothing

Reliable Set-Reset operation

up to <u>20 Gbits/s</u>

Limit depends on coding

and energy

Fast pulse response and Scaling Down Laser Size

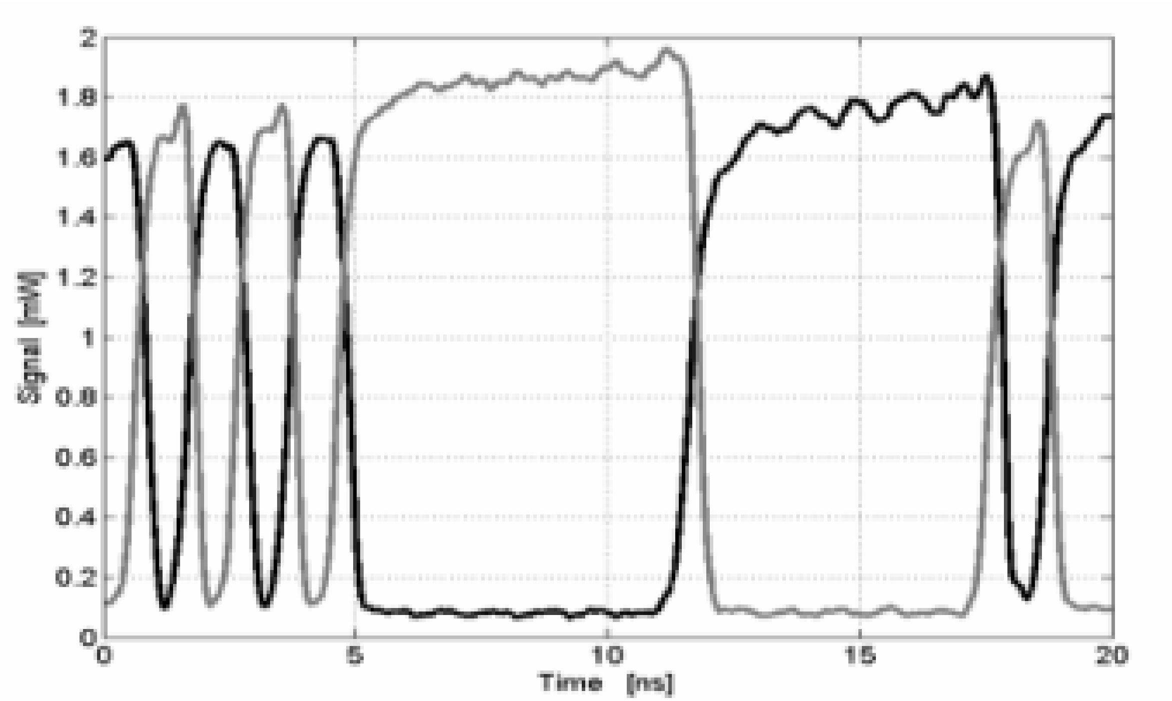

1 = Flip-Flop

0 = Nothing

Experimental Results

(5ps Pulses , 1 Gbit/s)

Reliable Set-Reset operation

up to 20 Gbits/s

Limit depends on coding

and energy

- **Minimal Pulse Energy to trigger the reversal**
- **Large Pulse Energies induce Relaxation Oscillations**
- **Shorter Pulses may encompass several modes**
- **Detuning is important for slow pulses**
- **Shorter devices don’t give an immediate improvement**
- **Set-Reset at 20 Gbit/s seems an attainable regime**
- **Rise time is governed by pulse width & pulse energy**

PUBLICATIONS

NOISE SPECTRA OF A SEMICONDUCTOR RING LASER IN THE BIDIRECTIONAL REGIME

Pérez-Serrano,Antonio;Zambrini,Roberta;Scirè,Alessandro;Colet,Pere
Submitted to Physical Review A , (2009)

■ SRL Model including spontaneous emission noise

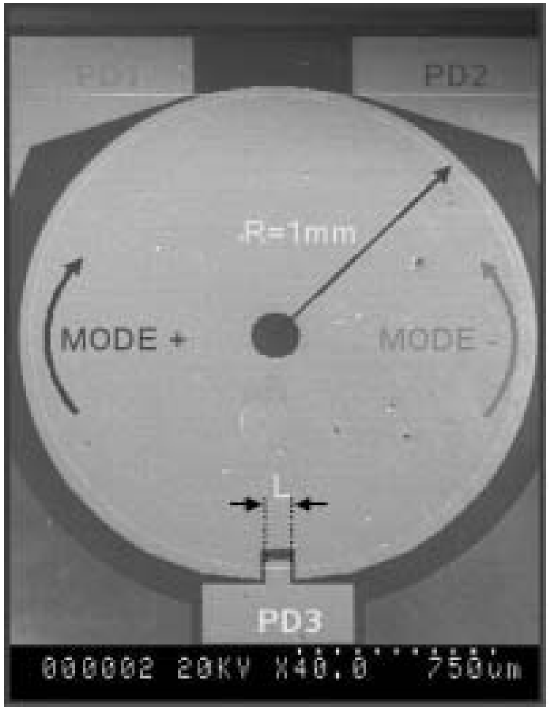

$$\begin{cases} \dot{E}_\pm(t) = \mathcal{G}_\pm(N(t), |E_\pm(t)|^2)\ E_\pm(t) - \eta\ E_\mp(t) + \xi_\pm(t) \\ \dot{N}(t) = \gamma\ \mathcal{F}(N(t), |E_\pm(t)|^2) \end{cases}$$

$$\mathcal{G}_\pm(N(t), |E_\pm(t)|^2) = \frac{1}{2}(1 + i\alpha)\{N(t)\ \sigma_\pm - 1\}$$

$$\mathcal{F}(N(t), |E_\pm(t)|^2) = \mu - N(t) - N(t)\ \sigma_+\ |E_+(t)|^2 - N(t)\ \sigma_-\ |E_-(t)|^2$$

$$\sigma_\pm = 1 - s\ |E_\pm(t)|^2 - c\ |E_\mp(t)|^2$$

$$\eta = k_d + ik_c$$

$$\langle \xi_\pm(t)\xi^*_\pm(t') \rangle = 2D\delta(t - t')$$
$$\langle \xi_\pm(t)\xi^*_\mp(t') \rangle = \langle \xi_\pm(t)\xi_\pm(t') \rangle = 0$$

$$\langle \xi_\pm(t)\xi^*_\pm(t') \rangle = 2\sqrt{\beta\tau_p N_{st}}\delta(t - t')$$

Linear Fluctuations Dynamics

$$E_{\pm}(t) = (Q + a_{\pm}(t))e^{i\omega t \pm i\phi} \qquad N(t) = \bar{N} + n(t)$$

Variable change → Block diagonalization

$$S(t) = a_{+}(t) + a_{-}(t)$$

$$R(t) = a_{+}(t) - a_{-}(t)$$

$$\begin{pmatrix} \dot{S}(t) \\ \dot{S}^{*}(t) \\ \dot{n}(t) \\ \dot{R}(t) \\ \dot{R}^{*}(t) \end{pmatrix} = \begin{pmatrix} \text{3 x 3} & & & 0 & 0 \\ & & & 0 & 0 \\ & & & 0 & 0 \\ 0 & 0 & 0 & \text{2 x 2} & \\ 0 & 0 & 0 & & \end{pmatrix} \begin{pmatrix} S(t) \\ S^{*}(t) \\ n(t) \\ R(t) \\ R^{*}(t) \end{pmatrix} + \begin{pmatrix} \xi_S^{*}(t) \\ \xi_S(t) \\ 0 \\ \xi_R(t) \\ \xi_R^{*}(t) \end{pmatrix}$$

Physical interpretation:

- *Re(S) ≡ I* → Total intensity
- *Re(R) ≡ D* → Intermodal power exchange

D-Spectrum: Numerical and Analytical

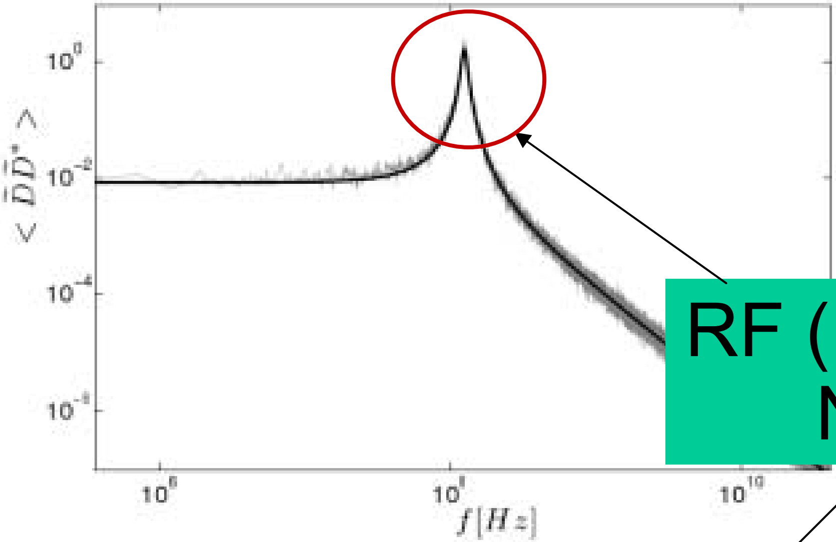

D-Spectrum depending on Kc

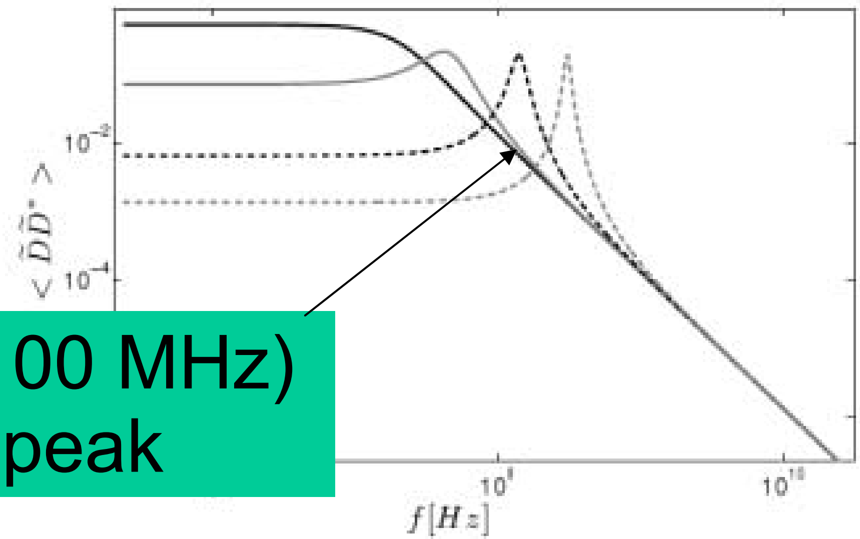

RF (10 – 100 MHz)
Noise peak

$k_c = 10^{-3}$; $k_c = 1.83\ 10^{-3}$; $k_c = 4.83\ 10^{-3}$; $k_c = 10^{-2}$

D-Spectrum depending on μ

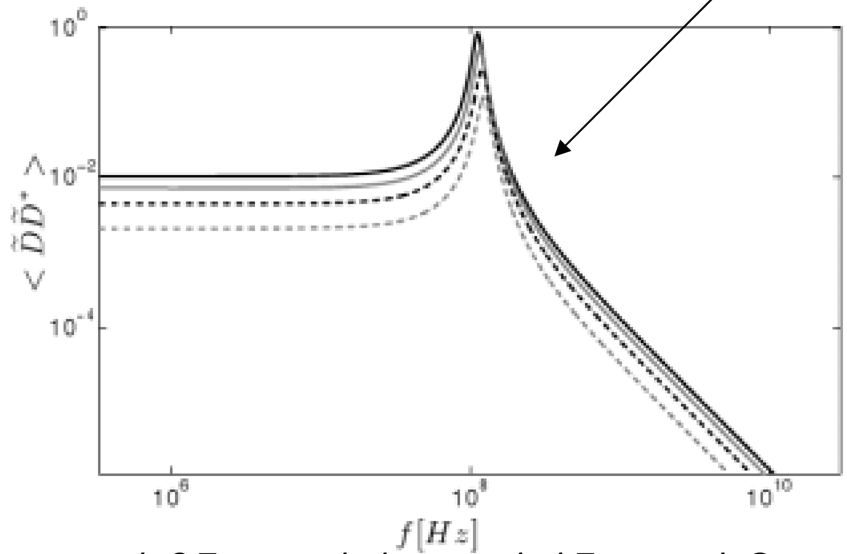

$\mu = 1.05$; $\mu = 1.1$; $\mu = 1.15$; $\mu = 1.2$

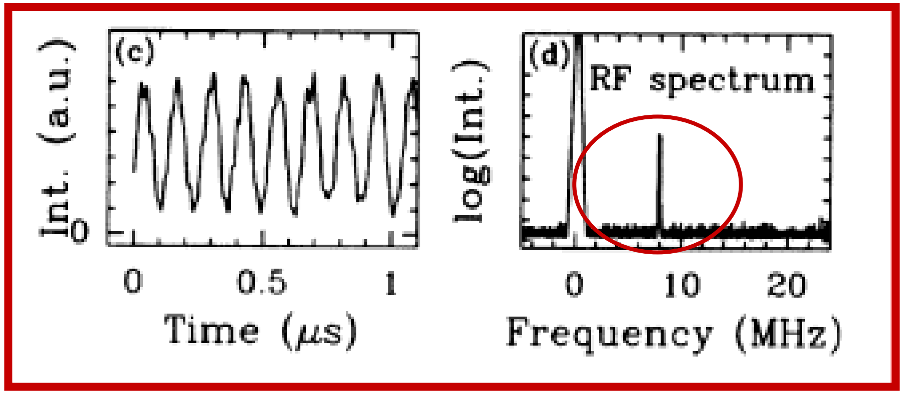

Ballantine et al APL 2000

IFISC

PUBLICATIONS

TOPOLOGICAL INSIGHT INTO THE NON-ARRHENIUS MODE HOPPING OF SEMICONDUCTOR RING LASERS

Beri,S.; Gelens,L.; Mestre, M.; Van der Sande, G.; Verschaffelt, G.; Scirè, A.; Mezosi, G. , Sorel, M.; Danckaert, J.
Physical Review Letters **101**, 093903 (1-4) (2008)

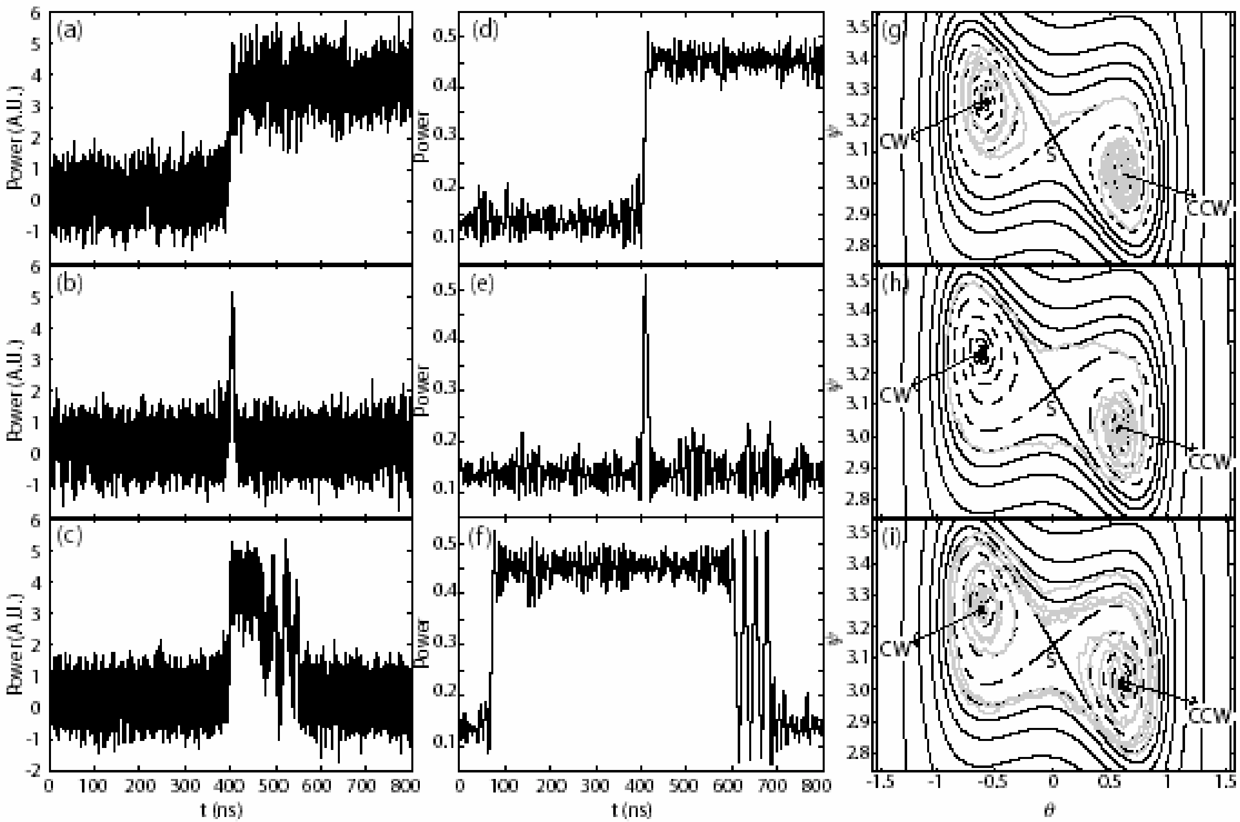

FIG. 2: Comparison between measured time series (a)-(c), simulated time series (d)-(f) and phase space trajectories (g)-(i) for different kind of transitions. In the experiment the ring was biased at $J_{ring} = 39.86$mA; the waveguide was biased at 8.22mA and the temperature was 21.55° C. In the numerical simulation the following parameters were used: $\mu = 1.59$, $\alpha = 3.5$, $s = 0.005$, $c = 0.01$ $k = 0.44\text{ns}^{-1}$, $\phi_k = 1.5$, $D = 6.5 \cdot 10^{-5}$ ns^{-1}. The notation of (f)-(i) is as follow: CW, CCW are the stable states, S is the saddle; solid line: stable manifold of S, dashed line: unstable manifold of S, gray: projection of the time series (d)-(f).

Applications

PUBLICATIONS

THEORETICAL ANALYSIS OF A NEW TECHNIQUE FOR INERTIAL ROTATION SENSING USING A SEMICONDUCTOR RING LASER

Pérez-Serrano, A;Scire,A;
Photonics Technology Letters, vol. 21, issue 13, July 1 2009, pp. 917-919 , (2009)

THE RING LASER GYROSCOPE

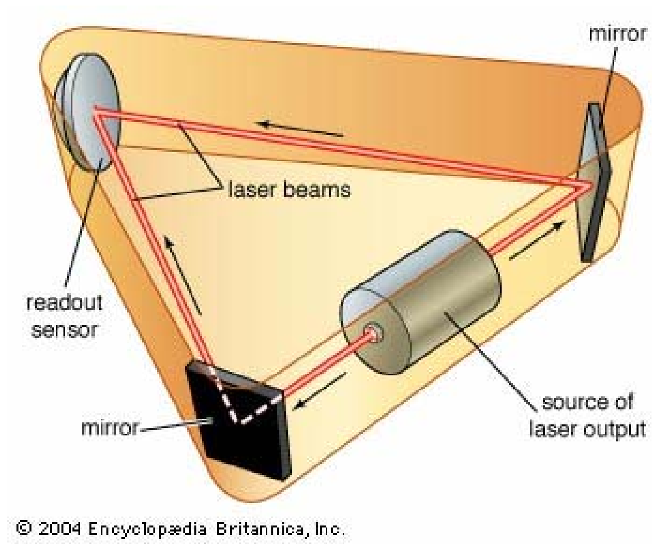

The change in path length generates a frequency shift

$$\Delta\upsilon = 4A\Omega / p\lambda$$

A: area
p: perimeter
λ: laser wavelength

Because of backscattering the counterpropagating modes are coupled at low rotation rates

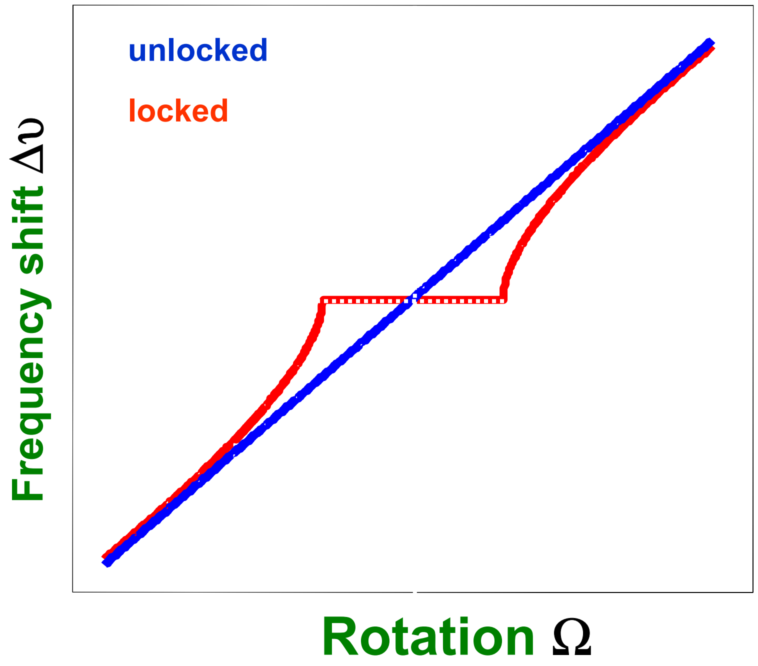

The locking frequency is proportional to the mode coupling strength

$$\Delta\upsilon = 4A\Omega/p\lambda = R\Omega$$

Not respected at low rotation rates

IFISC

■ SRL Gyroscope modeling

$$\dot{E}_{\pm}(t) = \mathcal{G}_{\pm}(N(t), |E_{\pm}(t)|^2)\; E_{\pm}(t) - \eta\; E_{\mp}(t) \pm i\Delta E_{\pm}(t),$$
$$\dot{N}(t) = \gamma\; \mathcal{F}(N(t), |E_{\pm}(t)|^2),$$

$$\mathcal{G}_{\pm}(N(t), |E_{\pm}(t)|^2) = \frac{1}{2}(1 + i\alpha)\{N(t)\;\sigma_{\pm} - 1\},$$

$$\mathcal{F}(N(t), |E_{\pm}(t)|^2) = \mu - N(t) - N(t)\;\sigma_{+}\;|E_{+}(t)|^2 - N(t)\;\sigma_{-}\;|E_{-}(t)|^2,$$

$$\sigma_{\pm} = 1 - s\;|E_{\pm}(t)|^2 - c\;|E_{\mp}(t)|^2,$$

$$\eta = k_d + ik_c$$

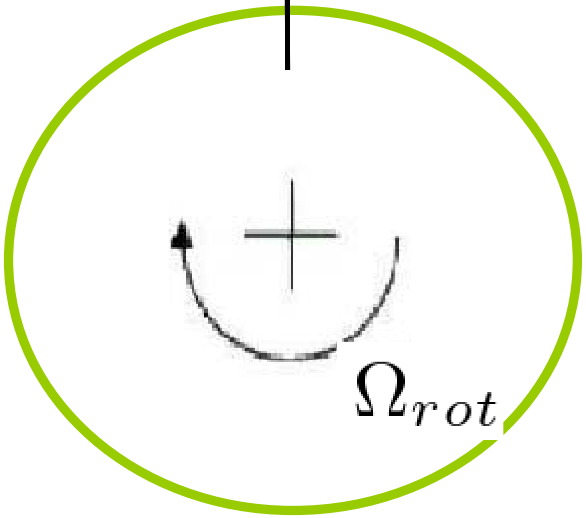

$$E_{\pm}(t) = Q_{\pm}e^{i(\omega t \pm \psi/2)},\;\; N(t) = \bar{N}.$$

$$\Delta = \frac{2\pi R\tau_p}{\lambda}\Omega_{rot}$$

■ SRL Responsivity to inertial rotation

$$\chi = \frac{|E_-|^2 - |E_+|^2}{|E_+|^2 + |E_-|^2} = \frac{2}{Q}\delta = \mathcal{R}\Omega_{rot} \quad \mathcal{R} = \frac{4\pi k_c R \tau_p}{\lambda(2k_d^2 + 2k_c^2 - (k_d + \alpha k_c)Q^2 \bar{N}(s-c))}$$

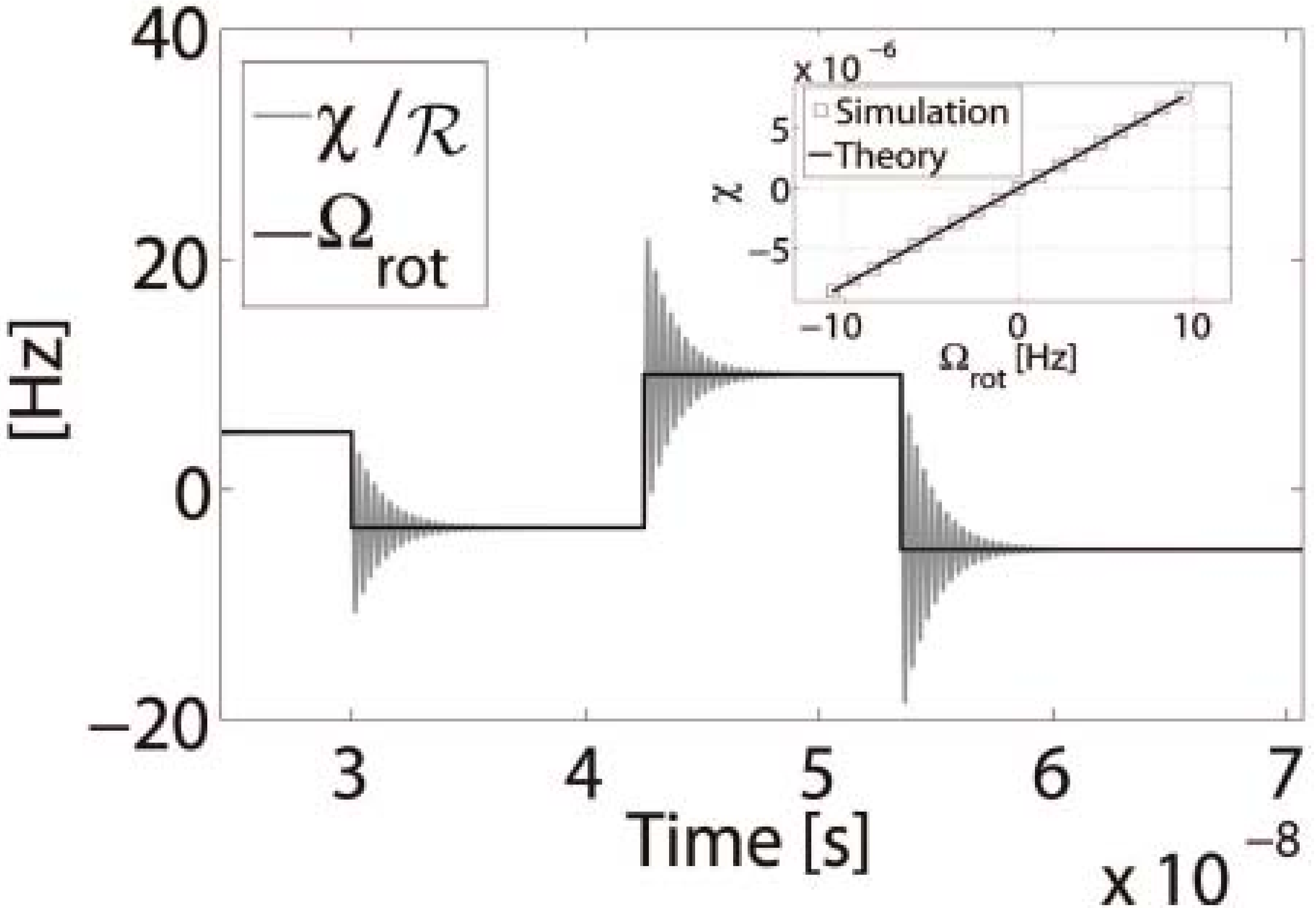

■ SRL Gyroscope – Experiments

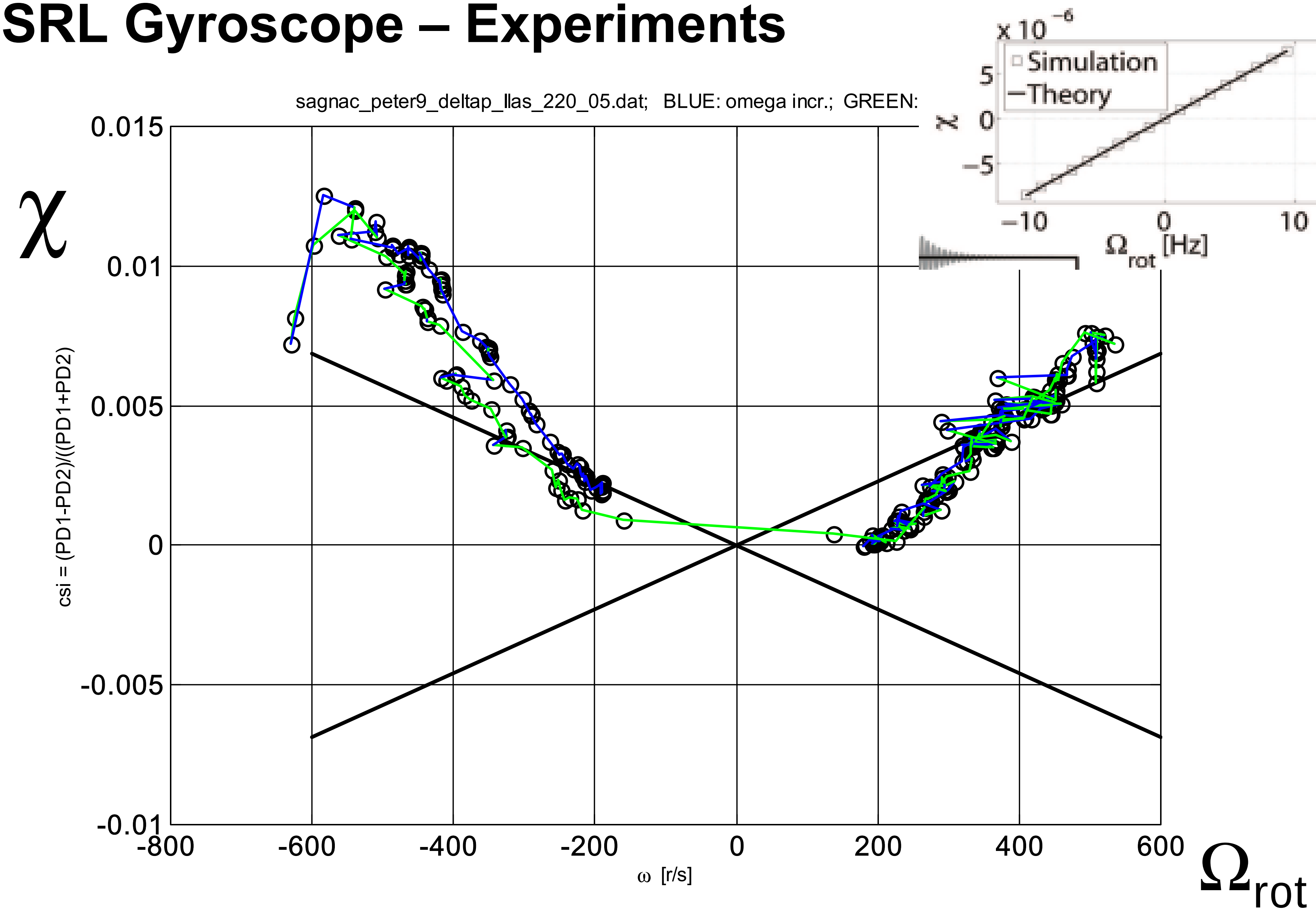

Bistable SRL as a possible generator of optical random bits by current modulation

A.Scirè, A.Perèz-Serrano, G.VanDerSande, J.Danckaert

In progress…

IDEA: In Bi-SRLs the laser switch-on mechanism itself provides a non-linear fast amplification of the noisy seed of the spontaneous emission. Being spontaneous emission isotropic, the probability that each spontaneously emitted photon is coupled to the cw (resp. ccw) mode is ½ for fundamental reasons. So, when the laser switches on due to current modulation towards the bistable region, cw or ccw mode will be activated with the same probability. However, fluctuations in such process lead the directional mode selection to be a stochastic process itself, in which microscopic fluctuations are brought to a macroscopic level during the laser switch on.

Sp. emission

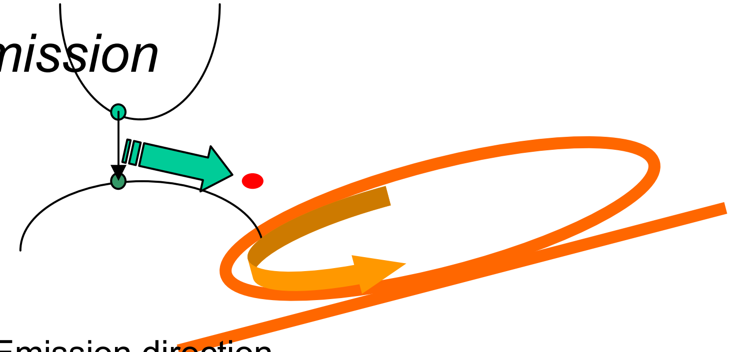

Emission direction
randomly affected by spontaneous emission
during SRL switch on

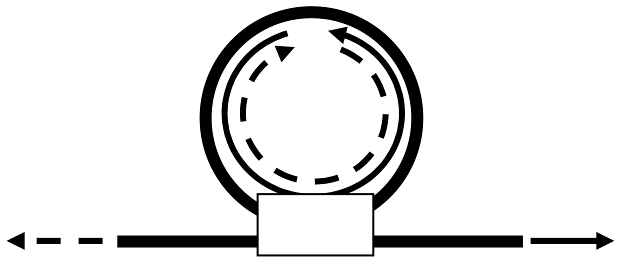

Solid arrow:
Counter-clockwise
mode

Dashed arrow:
Clockwise mode

- **Random Bits Generator, with simulations**
  Two-mode Rate Equations

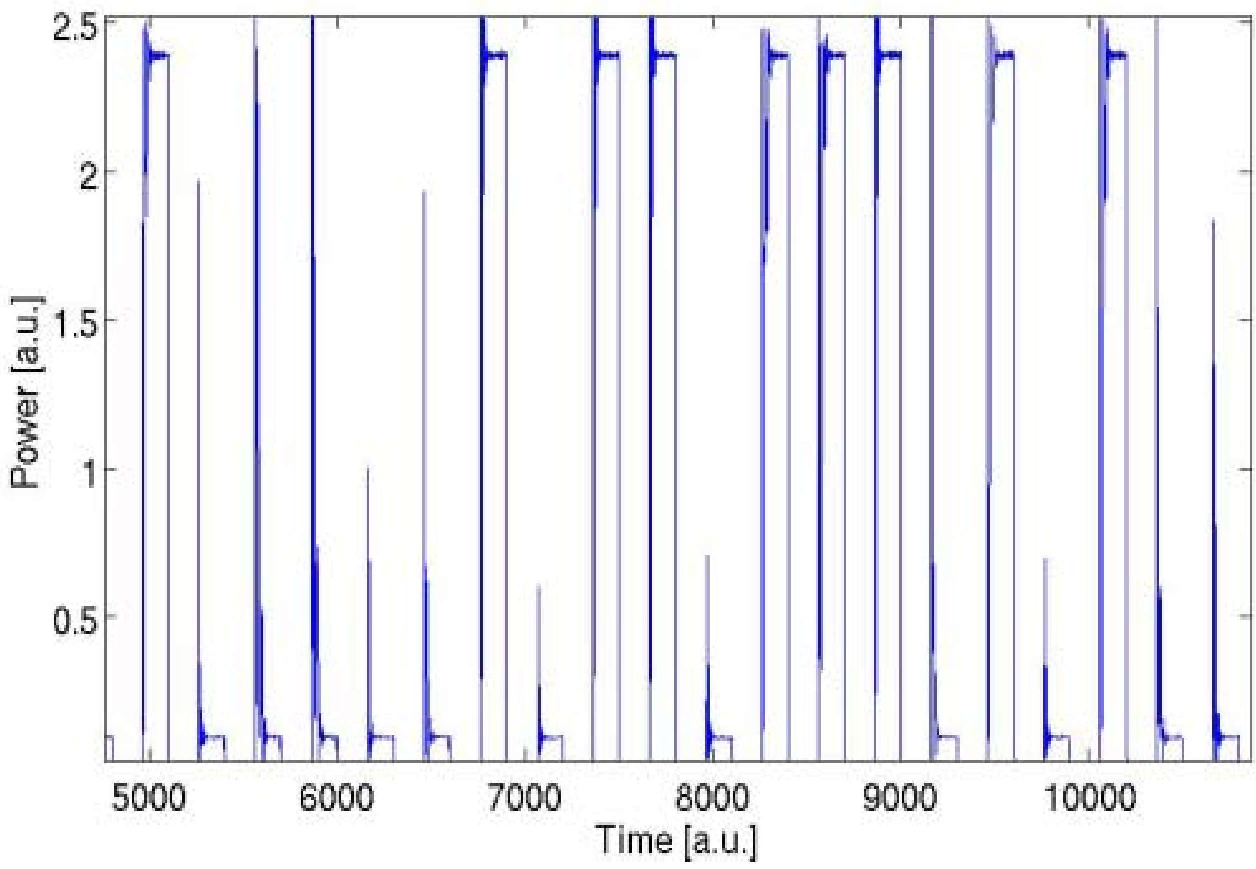

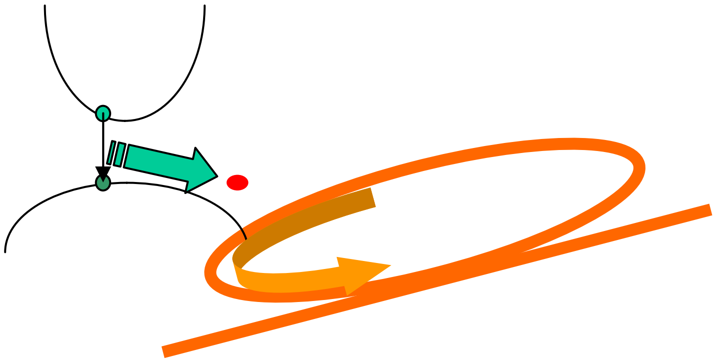

Electronic noise based RNGs (today produced and sold by INTEL) primarily sample thermal noise by amplifying the voltage measured across undriven resistors. The architecture is called *Dual Oscillator*

The thermal noise source is used to modulate the frequency of the slower clock. The variable, noise-modulated slower clock is used to trigger measurements of the fast clock. Drift between the two clocks thus provides the source of random binary digits.

[Velichko, S. "Random-number Generator Prefers Imperfect Clocks." *EDN Access*, 1996. (http://ednmag.com/reg/1996/112196/23_di04.cfm). Hoffman, Eric. *Random Number Generator*, 1996, U.S. Patent 5,706,208].

In the optical domain, existing RNGs are based on single-photon statistics (SPS) at a (ideally) 50% optical beam splitter

SPS take profit of the quantum discretization of light, so they need to operate in a range of optical power at which such discretization is visible, i.e. down to a single photon.

SPSs are limited in bandwith (MHz), bulky. SPS are produced and sold by QUANTIS

[US Patent 6393448, Deutche Telekom (2002); J.M. Mérolla et al., Single-Photon Interference in Sidebands of Phase-Modulated Light for Quantum Cryptography, Phys. Rev. Lett. 1656 (1999)].

IFISC

Quantum Random Number Generator

(PCI)

(USB)

(OEM)

When random numbers cannot be left to chance!

Although random numbers are required in many applications, their generation is often overlooked.

Being deterministic, computers are not capable of producing random numbers. A physical source of randomness is necessary. Quantum physics being intrinsically random, it is natural to exploit a quantum process for such a source. Quantum random number generators have the advantage over conventional randomness sources of being invulnerable to environmental perturbations and of allowing live status verification.

Quantis is a physical random number generator exploiting an elementary quantum optics process. Photons - light particles - are sent one by one onto a semi-transparent mirror and detected. The exclusive events (reflection - transmission) are associated to "0" - "1" bit values.

The operation of Quantis is continuously monitored. If a failure is detected the random bit stream is immediately disabled.

Quantis is available as a PCI card, an USB device and a component for mounting on a printed circuit board (see Quantis-OEM). Quantis is easily integrated in existing applications.

Main features

- True quantum randomness
- Passes NIST and Diehard randomness tests
- High bit rate up to 16 Mbits/s
- Low cost
- Compact and reliable
- Continuous status check
- Easy integration in existing applications

Applications

- Cryptography
- Gambling, lotteries
- Secure printing
- PIN number generation
- Mobile prepaid system
- Statistical research
- Numerical simulations

	Electronic RNG (Intel)	Single Photon RNG (Quantis)	Bi-SRL
RNG rate	KHz	MHz	GHz
Cost	Low	100-1000 Eu	?
Size	100-1000 mm^2	10-100 mm^2	1 mm^2
Output signal	Electrical	Electrical	Optical
Physical process behind randomness	Thermal noise in a resistor	Single photon transmission at a 50% beam splitters	Spontaneous emission noise


14 - 19 JUNE 2009
CLEO® EUROPE - EQEC 2009
CONFERENCE ON LASERS AND ELECTRO-OPTICS - EUROPEAN QUANTUM ELECTRONICS CONFERENCE
GENERAL
CONFERENCE
AUTHORS
SPEAKERS
SHORT COURSES
REGISTER
PROGRAM
CLEO®/Europe 2009 Invited Talks
Semiconductor Snail Lasers
M. J. Strain[1], A. Pérez-Serrano[2], G. Mezösi[1], G. Verschaffelt[3],
A. Scirè[2], J. Danckaert[3], M. Sorel[1], S. Balle[4]
1. University of Glasgow
2. IFISC (UIB-CSIC), Palma de Mallorca
3. Vrije Universiteit Brussel
4. IMEDEA (UIB-CSIC)

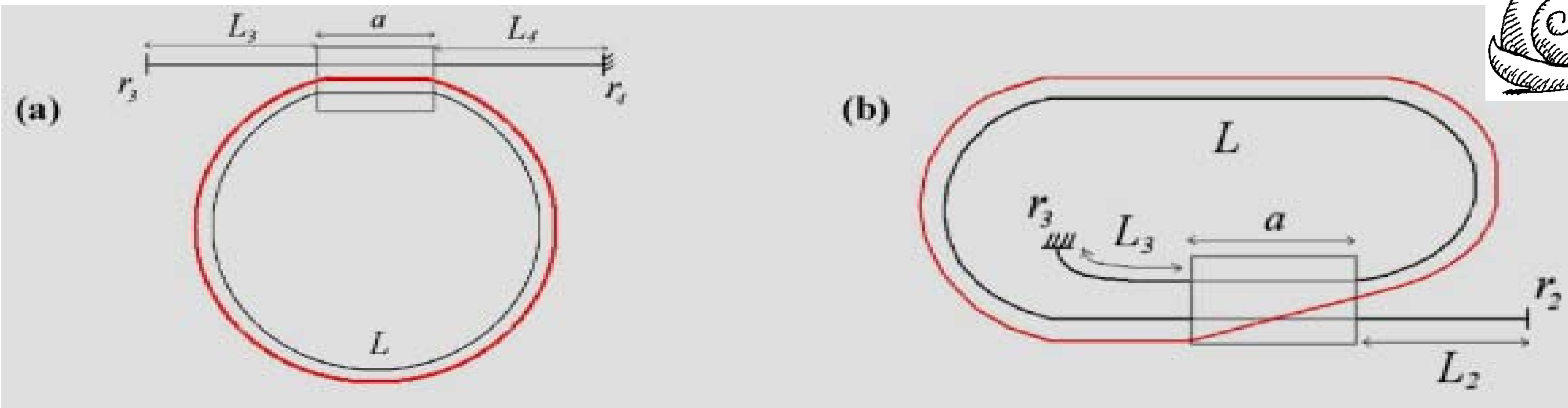

Fig. 1 (a) SRL schematic design. Output facet with reflectivity r_3 ($r_3 < r_4$). (b) Snail Laser schematic design. Output facet with reflectivity r_2 ($r_2 < r_3$). The waveguided of length L is pumped. The red line marks the resonant path.

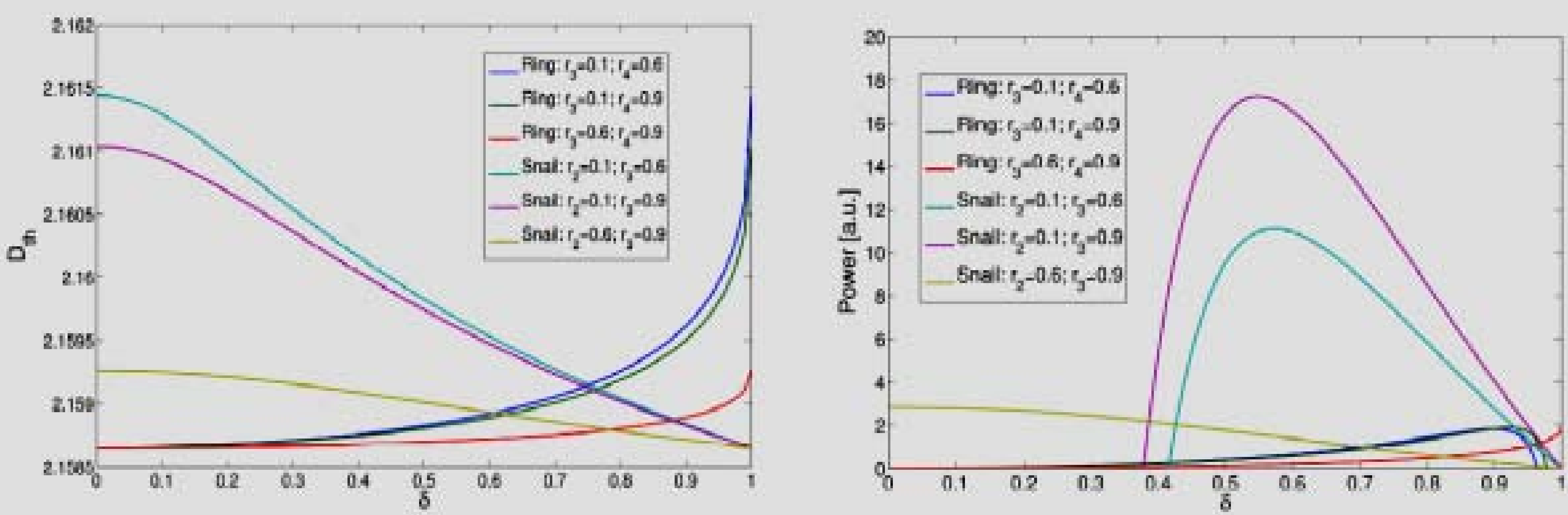

Fig. 2 (a) Carrier density threshold (D_{th}) vs Coupling efficiency (δ) for different parameter values and configurations. (b) Output Power vs Coupling efficiency (δ) for different parameter values and configurations.

Modes given by

$$Z_{\pm} = \frac{-i\delta(1+Z_2Z_3) \pm (1-\delta^2)\sqrt{Z_2Z_3}}{\delta^2 + Z_2Z_3}$$

$$Z = e^{iqL}$$

$$Z_2 = r_2 e^{2iq_2L_2}$$

$$Z_3 = r_3 e^{2iq_3L_3}$$

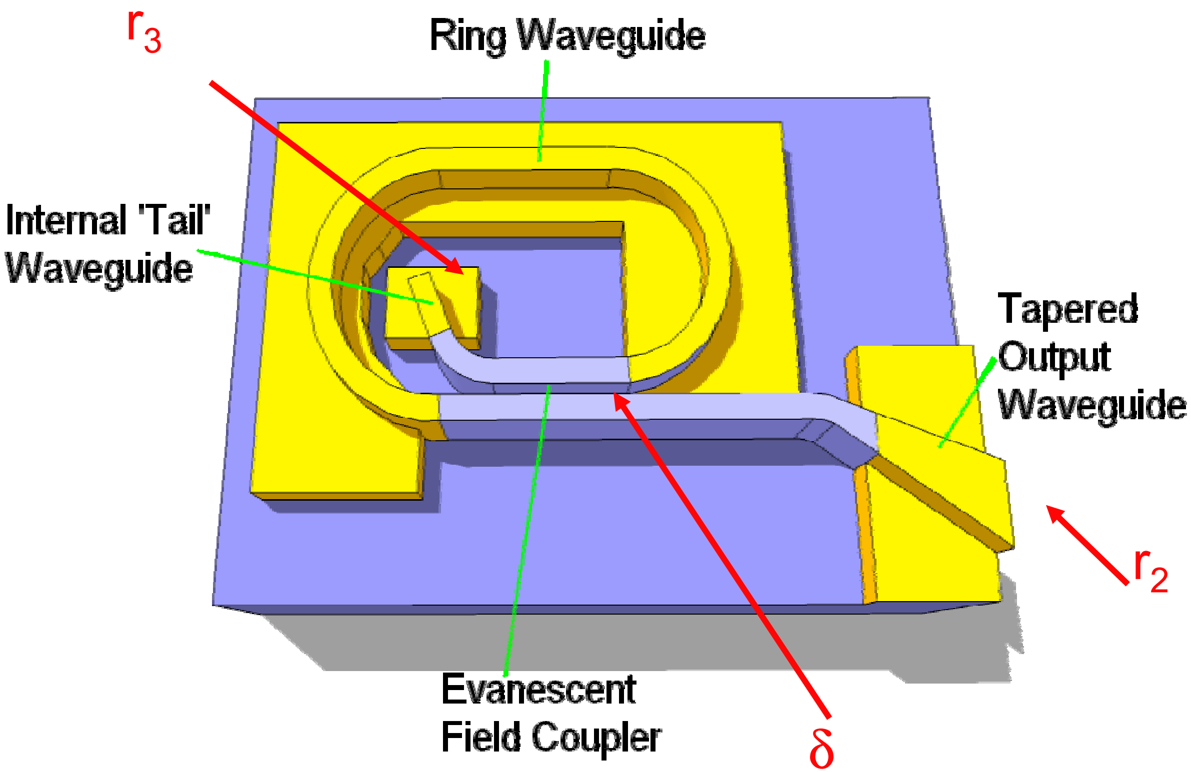

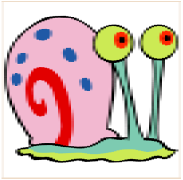

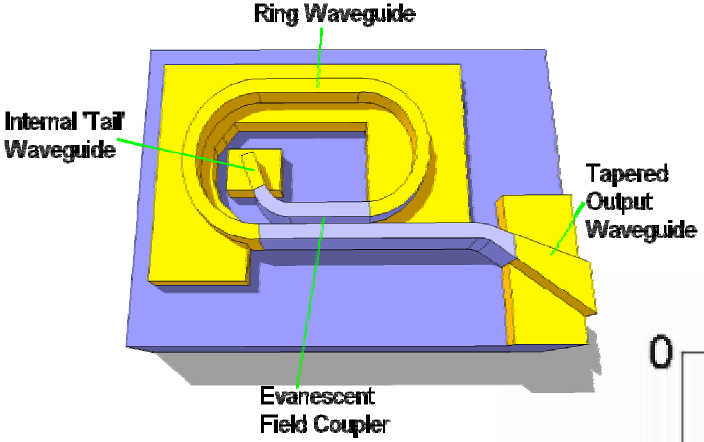

$$\Delta I m q_m^{\pm} = 2\frac{1-\delta^2}{\delta L}\sqrt{r_2 r_3}\cos\frac{q_3 L_3 + q_2 L_2}{2}$$

Loss modulation due to external waveguides

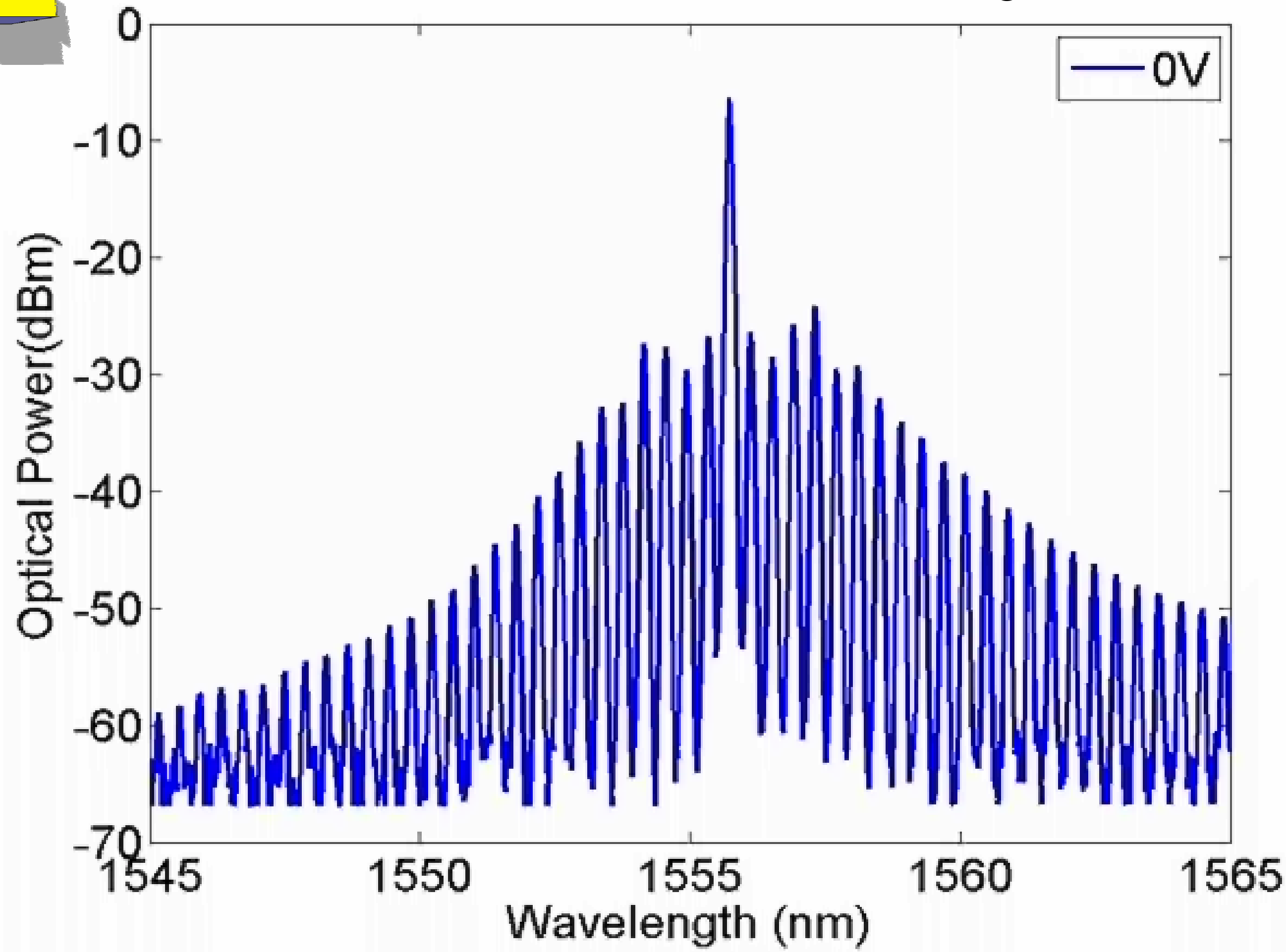

In progress

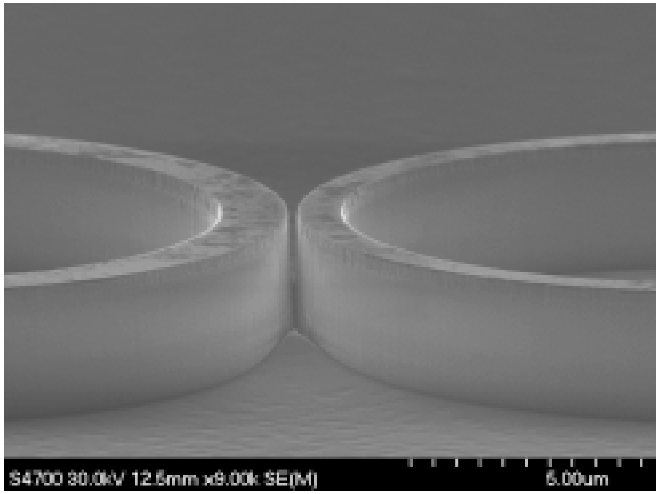

ACPHOM:
Active Photonic Molecules

a)

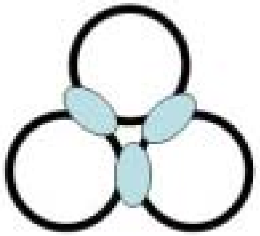

b)

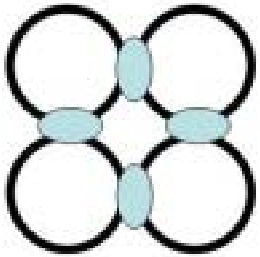

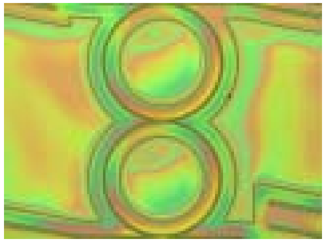

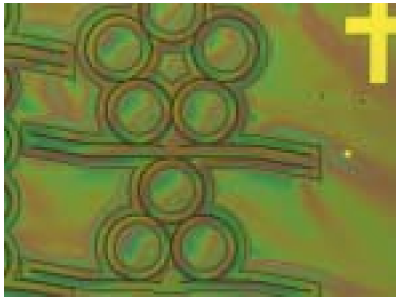

a)

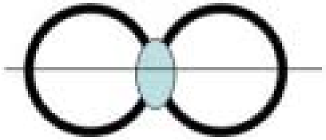

b)

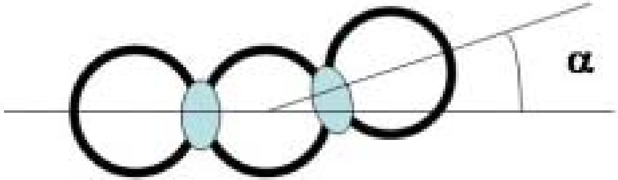

c)

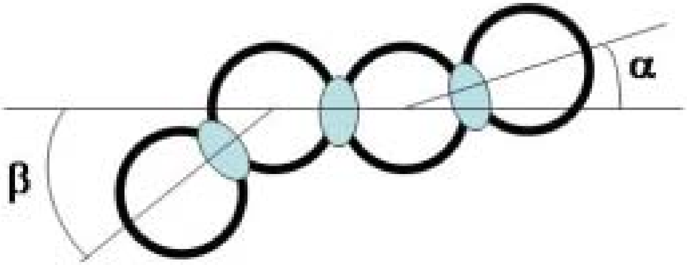

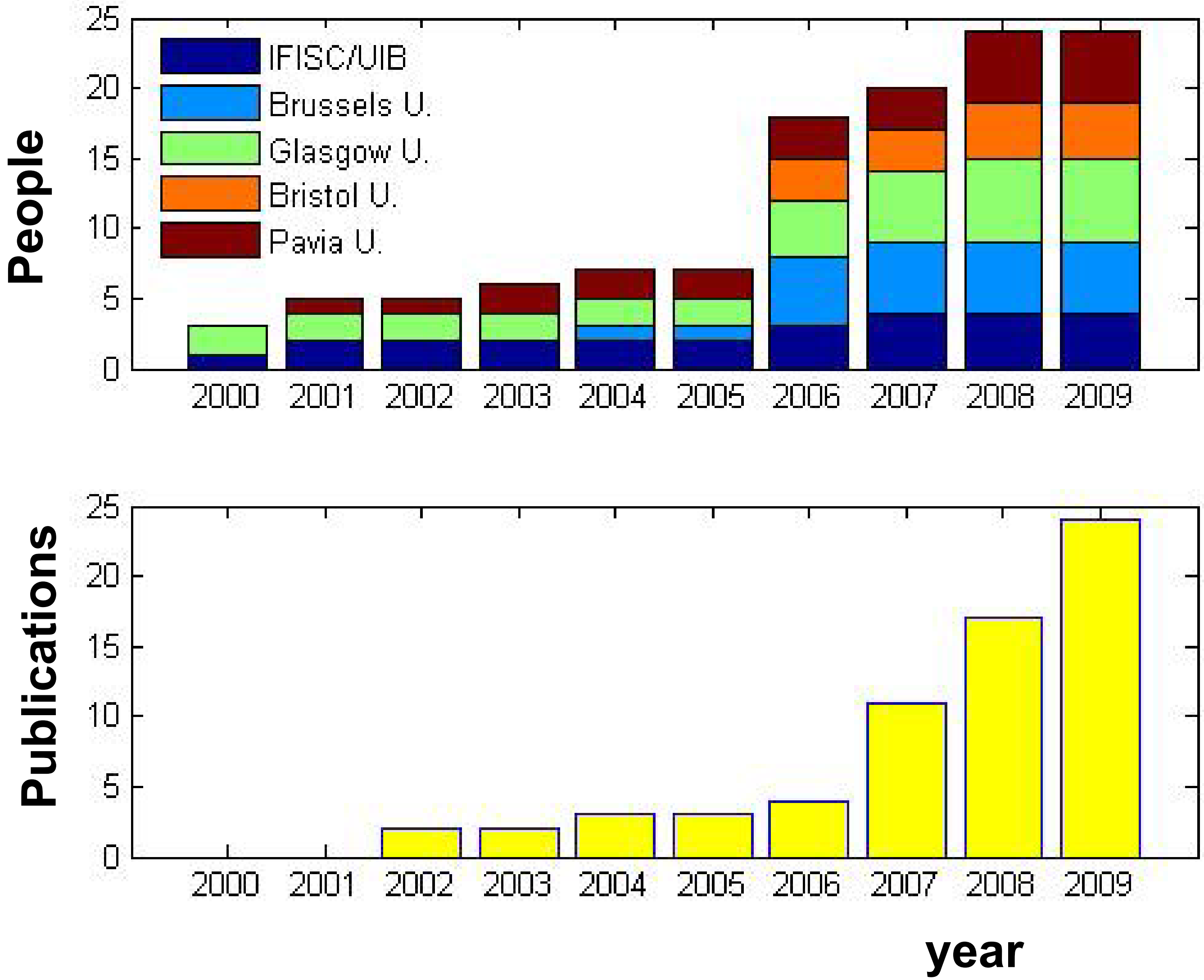
People
25
20
15
10
5
0
IFISC/UIB
Brussels U.
Glasgow U.
Bristol U.
Pavia U.
2000
2001
2002
2003
2004
2005
2006
2007
2008
2009
Publications
year

ACKNOWLEDGMENTS

SalvadorBalle

JulienJavaloyes

AntonioPérez-Serrano

RobertaZambrini,PereColet,MarcSorel, SandorFurst,GaborMezosi,MichaelStrain, GuidoGiuliani,RiccardoMiglierina,AndreaTrita, IlariaCristiani,FrancescaBragheri,SilvanoDonati, SiyuanYu,GououiYuan,BeiLi,ZouranWang, JanDanckaert,GuyVanDerSande, LendertGelens, GuyVerschaffelt,StefanoBeri, MichaelWale,DanYanson,JorgeCastro,JeanBuus, AngelaThreinhardt,MarkusKorn.

SEMICONDUCTOR RING LASER DYNAMICS

IOLOS tasks

- Modal Properties √
- TW-modelling √
- Directional switching √
- Noise properties
  - *Langevin formulation, noise spectra* √
  - *Mode hopping* √
- Applications
  - *Inertial rotation sensing* √
  - *Hardware Random Number Generation*
- New structures
  - *Snail laser*
  - *Active Photonic Molecules*